Electronic supplementary data to accompany

The shiny side of copper: Bringing copper(I) light-emitting electrochemical cells closer to application

Sarah Keller,[a] Alessandro Prescimone,[a] Maria-Grazia La Placa,[b] José M. Junquera-Hernández,[b] Henk J. Bolink,[b] Edwin C. Constable,[a] Michele Sessolo,*[b] Enrique Ortí*[b] and Catherine E. Housecroft*[a]

[a] Department of Chemistry, University of Basel, BPR 1096, Mattenstrasse 24a, CH-4058 Basel, Switzerland; email: catherine.housecroft@unibas.ch
[b] Instituto de Ciencia Molecular, Universidad de Valencia, 46980 Paterna (Valencia), Spain; email: enrique.orti@uv.es

Contents

1. Experimental

1.1. General

^{1}H, ^{13}C and ^{31}P NMR spectra were recorded at room temperature using Bruker Avance III-600, III-500 or III-400 NMR spectrometers. ^{1}H and ^{13}C NMR chemical shifts were referenced to residual solvent peaks with respect to δ(TMS) = 0 ppm, and ^{31}P NMR chemical shifts with respect to δ(85% aqueous H_3PO_4) = 0 ppm. Solution absorption and emission spectra were measured using an Agilent 8453 spectrophotometer and a Shimadzu RF-5301PC spectrofluorometer, respectively. Electrospray ionization (ESI) mass spectra were recorded on a Bruker esquire 3000plus or Shimadzu LCMS-2020 instrument. Quantum yields for CH_2Cl_2 solution and powder samples were measured using a Hamamatsu absolute photoluminescence (PL) quantum yield spectrometer C11347 Quantaurus-QY. Emission lifetimes and powder emission spectra were measured with a Hamamatsu Compact Fluorescence lifetime Spectrometer C11367 Quantaurus-Tau, using an LED light source with λ_{exc} = 365 nm. Thin films were analyzed using a Xe lamp coupled to a monochromator as the excitation source and an integrated sphere coupled to a spectrometer (Hamamatsu C9920-02 with a Hamamatsu PMA-11 optical detector) in order to quantitatively determine the PLQY. Low temperature emission and lifetime experiments were performed using an LP920-KS instrument from Edinburgh Instruments. 410 nm excitation was obtained from pulsed third-harmonic radiation from a Quantel Brilliant b Nd:YAG laser equipped with a Rainbow optical parameter oscillator (OPO). The laser pulse duration was ~10 ns and the pulse frequency 10 Hz, with a typical pulse energy of 7 mJ. Detection of the spectra occurred on an iCCD camera from Andor. Single-wavelength kinetics were recorded using a photomultiplier tube.

1.2. Syntheses

2-Chloro-4,5,6-trimethylpyridine,[1] 2-*tert*-butyl-6-chloropyridine[2] and $[Cu(MeCN)_4][PF_6]$[3] were synthesized using literature methods and the spectroscopic data matched those reported. POP was purchased from Acros, xantphos from Fluorochem, and 6,6'-dimethyl-2,2'-bipyridine (6,6'-Me_2bpy) and 5,5'-dimethyl-2,2'-bipyridine (5,5'-Me_2bpy) from Sigma-Aldrich. All chemicals were used as received.

6-(*tert*-Butyl)-2,2'-bipyridine (6-*t*Bubpy), 2-*tert*-butyl-6-chloropyridine (420 mg, 2.48 mmol), 2-pyridinylzinc bromide (7.4 mL, 0.5 M in THF, 3.7 mmol) and $[Pd(PPh_3)_4]$ (218 mg, 0.19 mmol, 7.1 mol%) were weighed into a microwave vial under argon together with degassed THF (7 mL). The vial was then heated in the microwave reactor (4h, 110 °C, medium absorption) and purified by chromatography on a silica column (cyclohexane-EtOAc, 4:1). The product was obtained as a colourless oil (268 mg, 1.26 mmol, 51 %). The ^{1}H NMR spectrum matched that reported in the literature.[4]

4,5,6-Trimethyl-2,2'-bipyridine (4,5,6-Me_3bpy), 2-chloro-4,5,6-trimethylpyridine (2.17 g, 13.9 mmol), 2-pyridinylzinc bromide (42 mL, 0.5 M in THF, 21 mmol) and $[Pd(PPh_3)_4]$ (1.16 g, 1.0 mmol, 6.7 mol%) were weighed into a flask under argon with degassed THF (20 mL) and stirred overnight. The workup was performed according to the general procedure reported in the literature for similar compounds.[5] After having been stirred overnight, the mixture was poured into an aqueous EDTA/Na_2CO_3 solution. Upon dissolution of the precipitate, the mixture was extracted with Et_2O (4 × 70 mL), and dried over Na_2SO_4. All volatiles were removed *in vacuo*, the residue was purified by chromatography on an alumina column (neutral, hexane:EtOAc gradient) and the product was obtained as a colourless oil in modest yield (0.106 g, 0.53 mmol, 4 %). ESI MS: *m/z* 199.1 $[M+H]^+$ (base peak, calc. 199.1). ^{1}H NMR

(500 MHz, 298 K, $CDCl_3$) δ/ppm: 8.65 (ddd, J = 4.8, 1.8, 0.9 Hz, 1H, H^{A6}), 8.38 (dt, J = 8.0, 1.1 Hz, 1H, H^{A3}), 8.00 (s, 1H, H^{B3}), 7.77 (td, J = 7.7, 1.8 Hz, 1H, H^{A4}), 7.25 (ddd, J = 7.7, 4.9, 1.1, Hz, 1H, H^{A5}), 2.60 (s, 3H, Me^{B6}), 2.36 (s, 3H, Me^{B4}), 2.25 (s, 3H, Me^{B5}). ^{13}C NMR (126 MHz, 298 K, $CDCl_3$) δ/ppm: 156.9 (C^{A2}), 156.3 (C^{B2}), 152.3 (C^{B4}), 149.1 (C^{A6}), 146.2 (C^{B6}), 136.9 (C^{A4}), 130.7 (C^{B5}), 123.2 (C^{A5}), 121.0 (C^{A3}), 120.3 (C^{B3}), 23.6 (Me^{B6}), 20.2 (Me^{B4}), 14.9 (Me^{B5}). Found: C 77.97, H 7.01, N 13.39; $C_{13}H_{14}N_2$ requires C 78.75, H 7.12, N 14.13.

2-Ethyl-1,10-phenanthroline (2-Etphen), In a 250 mL three-necked round-bottom flask under nitrogen and equipped with a condenser, 1,10-phenanthroline (1.982 g, 11 mmol) was dissolved in dry THF (50 mL) and the colourless solution cooled to −78 °C. A solution of ethyllithium (56 mL, 0.5 M in cyclohexane, 28 mmol, 2.5 eq) was slowly added via syringe, resulting in a colour change to dark red. The reaction mixture was stirred overnight, allowing it to warm to room temperature (RT). After refluxing the reaction mixture for 4 h, it was then cooled first to RT and then in an ice bath. A mixture of water and ice (100 mL) was added and the slurry stirred for 15 min. The organic solvents (THF and cyclohexane) were evaporated using a rotary evaporator. The aqueous phase was extracted with CH_2Cl_2 (5 × 50 mL). All organic phases were combined and dried over $MgSO_4$. While cooling in an ice bath, MnO_2 (30 g, 345 mmol) was added and the mixture was stirred for 45 min. After filtration over silica, all solvents were removed in vacuo to yield a yellow oil, which was purified by column chromatography (Silica pentane-EtOAc 99:1 – 80: 20, 1–2 % NEt_3). The title compound was obtained as a colourless oil (121 mg, 0.6 mmol, 5%) and the NMR spectroscopic data matched that previously reported.[6] ^{1}H NMR (500 MHz, $CDCl_3$, 298 K) δ/ppm: 9.21 (dd, J = 4.3, 1.8 Hz, 1H, H^{B9}), 8.22 (dd, J = 8.1, 1.8 Hz, 1H, H^{B7}), 8.17 (d, J = 8.2 Hz, 1H, H^{B4}), 7.76 (d, J = 8.8 Hz, 1H, H^{B5}), 7.72 (d, J = 8.8 Hz, 1H, H^{B6}), 7.60 (dd, J = 8.0, 4.3 Hz, 1H, H^{B8}), 7.56 (d, J = 8.2 Hz, 1H, H^{B3}), 3.26 (q, J = 7.7 Hz, 2H, $H^{Et\text{-}CH2}$), 1.46 (t, J = 7.7 Hz, 3H, $H^{Et\text{-}CH3}$). ^{13}C NMR (126 MHz, $CDCl_3$, 298 K) δ/ppm: 164.8 (C^{B2}), 150.4 (C^{B9}), 146.3 (C^{B10a}), 145.8 (C^{B10b}), 136.5 (C^{B4}), 136.1 (C^{B7}), 128.9 (C^{B6a}), 127.0 (C^{B4a}), 126.6 (C^{B5}), 125.6 (C^{B3}), 122.8 (C^{B8}), 122.4 (C^{B3}), 32.7 ($C^{Et\text{-}CH2}$), 14.7 ($C^{Et\text{-}CH3}$).

[Cu(POP)(5,5'-Me_2bpy)][PF_6], A colourless solution of [Cu($MeCN)_4$][PF_6] (93 mg, 0.25 mmol) and POP (134 mg, 0.25 mmol) in CH_2Cl_2 (40 mL) was stirred for 2 h, after which 5,5'-Me_2bpy (46 mg, 0.25 mmol) was added and the yellow solution stirred for another 2 h. The solution was filtered and the solvent from the filtrate was removed in vacuo. The yellow powder was redissolved in CH_2Cl_2 and layered with Et_2O. This gave yellow crystals, which were powdered and washed with hexane, giving [Cu(POP)(5,5'-Me_2bpy)][PF_6] in good yield (160 mg, 0.17 mmol, 69%). ^{1}H NMR (500 MHz, $(CD_3)_2CO$, 298 K) δ/ppm: 8.41 (d, J = 8.4 Hz, 2H, H^{B3}), 8.40–8.38 (m, 2H, H^{B6}), 7.91 (m, 2H, H^{B4}), 7.45–7.41 (m, 2H, H^{C5}), 7.38 (t, J = 7.4 Hz, 4H, H^{D4}), 7.27 (t, J = 7.6 Hz, 8H, H^{D3}), 7.22 (dtd, J = 5.8, 3.1, 1.0 Hz, 2H, H^{C6}), 7.16–7.12 (m, 8H, H^{D2}), 7.09 (td, J = 7.5, 0.6 Hz, 2H, H^{C4}), 6.78 (dtd, J = 7.8, 4.3, 1.6 Hz, 2H, H^{C3}), 2.15 (s, 6H, $H^{bpy\text{-}Me}$). ^{13}C NMR (126 MHz, $(CD_3)_2CO$, 298 K) δ/ppm: 159.2 (C^{C1}), 150.7 (C^{B6}), 150.5 (C^{B2}), 139.8 (C^{B4}), 137.0 (C^{B5}), 135.0 (C^{C3}), 134.1 (t, J = 8.2 Hz, C^{D2}), 133.1 (C^{C5}), 131.9 (t, J = 17.1 Hz, C^{D1}), 131.0 (C^{D4}), 129.6 (t, J = 4.8 Hz, C^{D3}), 126.1 (t, J = 2.2 Hz, C^{C4}), 124.8 (t, J = 14.7 Hz, C^{C2}), 122.6 (C^{B3}), 121.5 (C^{C6}), 18.1 (CH_3). ^{31}P{^{1}H} NMR (202 MHz, $(CD_3)_2CO$, 298 K) δ/ppm: −11.1 (broad, FWHM = 305 Hz, POP), −144.2 (septet, J_{PF} = 708 Hz, $[PF_6]^-$). ESI MS: m/z 785.5 $[M–PF_6]^+$ (base peak, calc. 785.2). Found: C 60.63, H 4.49, N 3.19; $C_{48}H_{40}CuF_6N_2OP_3 \cdot H_2O$ requires C 60.73, H 4.46, N 2.95.

[Cu(xantphos)(5,5'-Me_2bpy)][PF_6], A colourless solution of xantphos (145 mg, 0.25 mmol) and 5,5'-Me_2bpy (46 mg, 0.25 mmol) in CH_2Cl_2 (20 mL) was added dropwise to a colourless solution of [Cu($MeCN)_4$][PF_6] (93 mg, 0.25 mmol) in CH_2Cl_2 (20 mL). After stirring for 2h, the yellow solution was filtered and the solvent was removed in vacuo. The yellow powder was redissolved in CH_2Cl_2 and

layered with Et_2O. This yielded yellow crystals, which were powdered and washed with hexane, giving [Cu(xantphos)(5,5'-Me_2bpy)][PF_6] in good yield (215 mg, 0.22 mmol, 88%). ^{1}H NMR (500 MHz, $(CD_3)_2CO$, 298 K) δ/ppm: 8.48 (d, J = 9.0 Hz, 2H, H^{B3}), 7.95 (m, 2H, H), 7.94 (m, 2H, H^{B4}), 7.89 (dd, J = 7.8, 1.4 Hz, 2H, H^{C5}), 7.35–7.31 (m, 4H, H^{D4}), 7.28 (t, J = 7.7 Hz, 2H, H^{C4}), 7.22–7.18 (m, 8H, H^{D3}), 7.07–7.02 (m, 8H, H^{D2}), 6.55–6.51 (m, 2H, H^{C3}), 2.10 (s, 6H, $H^{bpy\text{-}Me}$), 1.83 (s, 6H, $H^{xantphos\text{-}Me}$). ^{13}C NMR (126 MHz, $(CD_3)_2CO$, 298 K) δ/ppm: 155.9 (t, J = 6.2 Hz, C^{C1}), 150.5 (t, J = 2.1 Hz, C^{B2}), 150.2 (C^{B6}), 140.1 (C^{B4}), 137.2 (C^{B5}), 135.1 (t, J = 1.5 Hz, C^{C6}), 133.8 (t, J = 8.1 Hz, C^{D2}), 132.4 (t, J = 17.2 Hz, C^{D1}), 132.0 (C^{C3}), 130.9 (C^{D4}), 129.7 (t, J = 4.8 Hz, C^{D3}), 128.4 (C^{C5}), 126.2 (t, J = 2.4 Hz, C^{C4}), 122.9 (C^{B3}), 120.8 (t, J = 13.7 Hz, C^{C2}), 37.0 (t, J = 1.5 Hz, $C^{xantphos\text{-}bridge}$), 28.3 ($C^{xantphos\text{-}Me}$), 18.0 ($C^{bpy\text{-}Me}$). ^{31}P NMR (162 MHz, $(CD_3)_2CO$, 294 K) δ/ppm: –11.6 (broad, FWHM = 230 Hz, xantphos), –144.2 (septet, J_{PF} = 708 Hz, $[PF_6]^-$). ESI MS: m/z 825.4 $[M–PF_6]^+$ (base peak, calc. 825.2). Found: C 62.87, H 4.77, N 3.26; $C_{51}H_{44}CuF_6N_2OP_3$ requires C 63.06, H 4.57, N 2.88.

[Cu(POP)(2-Etphen)][PF_6], A colourless solution of [Cu($MeCN)_4$][PF_6] (108 mg, 0.29 mmol) and POP (156 mg, 0.29 mmol) in CH_2Cl_2 (40 mL) was stirred for 2 h, after which 2-Etphen (60 mg, 0.29 mmol) was added and the yellow solution was stirred for another 2 h. The solution was filtered and the solvent from the filtrate was removed in vacuo. The yellow powder was redissolved in CH_2Cl_2 and layered with Et_2O. This yielded yellow crystals, which were powdered and washed with hexane, giving [Cu(POP)(2-Etphen)][PF_6] in good yield (247 mg, 0.26 mmol, 90%). ^{1}H NMR (500 MHz, $(CD_3)_2CO$, 298 K) δ/ppm: 9.12 (m, 1H, H^{B9}), 8.75 (d, J = 8.4 Hz, 1H, H^{B4}), 8.67 (dd, J = 8.2, 1.2 Hz, 1H, H^{B7}), 8.21 (d, J = 8.8 Hz, 1H, H^{B5}), 8.14 (d, J = 8.9 Hz, 1H, H^{B6}), 7.90 (d, J = 8.4 Hz, 1H, H^{B3}), 7.79 (dd, J = 8.2, 4.7 Hz, 1H, H^{B8}), 7.47 (ddd, J = 8.2, 7.5, 1.7 Hz, 2H, H^{C5}), 7.33 (q, J = 7.5 Hz, 4H, $H^{D4/D4'}$), 7.26 (m, 2H, H^{C6}), 7.23 (m, 4H, $H^{D3/D3'}$), 7.19 (m, 4H, $H^{D3/D3'}$), 7.16 (m, 4H, $H^{D2/D2'}$), 7.14 (td, J = 7.6, 1.0 Hz, 2H, H^{C4}), 7.01 (q, J = 6.1 Hz, 4H, $H^{D2/D2'}$), 6.86 (dtd, J = 7.8, 4.1, 1.6 Hz, 2H, H^{C3}), 2.99 (q, J = 7.7 Hz, 2H, $H^{Et\text{-}CH2}$), 0.75 (t, J = 7.7 Hz, 3H, $H^{Et\text{-}CH3}$). ^{13}C NMR (126 MHz, $(CD_3)_2CO$, 298 K) δ/ppm: 165.8 (C^{B2}), 159.0 (t, J = 6.0 Hz, C^{C1}), 150.7 (C^{B9}), 144.5 (C^{B10a}), 143.6 (C^{B10b}), 139.4 (C^{B4}), 138.7 (C^{B7}), 135.0 (C^{C3}), 134.2 (t, J = 7.6 Hz, $C^{D2/D2'}$), 133.7 (t, J = 7.4 Hz, $C^{D2/D2'}$), 133.2 (C^{C5}), 132.2 (t, J = 16.7 Hz, $C^{D1/D1'}$), 131.0 (d, J = 12.3 Hz, $C^{D4/D4'}$), 130.7 (C^{B6a}), 129.7 (m, $C^{D3/D3'}$), 129.1 (C^{B4a}), 128.1 (C^{B5}), 127.2 (C^{B6}), 126.1 (t, J = 2.2 Hz, C^{C4}), 125.6 (C^{B8}), 125.0 (d, J = 14.0 Hz, C^{C2}), 124.9 (C^{B3}), 121.3 (t, J = 1.8 Hz, C^{C6}), 34.8 ($C^{Et\text{-}CH2}$), 13.2 ($C^{Et\text{-}CH3}$). ^{31}P NMR (162 MHz, $(CD_3)_2CO$, 294 K) δ/ppm: –12.7 (broad, FWHM = 375 Hz, xantphos), –144.2 (septet, J_{PF} = 708 Hz, $[PF_6]^-$). ESI MS: m/z 809.4 $[M–PF_6]^+$ (base peak, calc. 809.2). Found: C 62.76, H 4.52, N 3.30; $C_{50}H_{40}CuF_6N_2OP_3$ requires C 62.86, H 4.22, N 2.93.

[Cu(xantphos)(2-Etphen)][PF_6], A colourless solution of xantphos (168 mg, 0.29 mmol) and 2-Etphen (60 mg, 0.29 mmol) in CH_2Cl_2 (20 mL) was added dropwise to a colourless solution of [Cu($MeCN)_4$][PF_6] (108 mg, 0.29 mmol) in CH_2Cl_2 (20 mL). After stirring for 2h, the yellow solution was filtered and the solvent was removed in vacuo. The yellow powder was redissolved in CH_2Cl_2 and layered with Et_2O. This yielded yellow crystals, which were powdered and washed with hexane, giving [Cu(xantphos)(2-Etphen)][PF_6] in good yield (259 mg, 0.26 mmol, 90%). ^{1}H NMR (500 MHz, $(CD_3)_2CO$, 298 K) δ/ppm: 9.10 (d, J = 4.3 Hz, 1H, H^{B9}), 8.76 (d, J = 8.4 Hz, 1H, H^{B4}), 8.68 (dd, J = 8.1, 1.1 Hz, 1H, H^{B7}), 8.20 (d, J = 8.9 Hz, 1H, H^{B5}), 8.12 (d, J = 8.9 Hz, 1H, H^{B6}), 7.90 (d, J = 5.8 Hz, 1H, H^{B3}), 7.89 (dd, J = 6.5, 1.3 Hz, 2H, H^{C5}), 7.88 (dd, J = 8.2, 4.7 Hz, 1H, H^{B8}), 7.41–7.36 (m, 2H, $H^{D4/D4'}$), 7.30 (m, 2H, H^{C5}), 7.29–7.24 (m, 8H, $H^{D2/D2'+D3/D3'}$), 7.20–7.16 (m, 2H, $H^{D4/D4'}$), 7.00–6.94 (m, 4H, $H^{D3/D3'}$), 6.79 (ddd, J = 8.3, 6.6, 3.2 Hz, 4H, $H^{D2/D2'}$), 6.71 (ddd, J = 7.5, 5.5, 2.4 Hz, 2H, H^{C3}), 2.59 (q, J = 7.7 Hz, 2H, $H^{Et\text{-}CH2}$), 1.99 (s, 3H, $H^{xantphos\text{-}CH3}$), 1.66 (s, 3H, $H^{xantphos\text{-}CH3}$), 0.57 (t, J = 7.7 Hz, 3H, $H^{Et\text{-}CH3}$). ^{13}C NMR (126 MHz, $(CD_3)_2CO$, 298 K) δ/ppm: 165.2 (C^{B2}), 155.9 (t, J = 6.3 Hz, C^{C1}), 150.4 (C^{B9}), 144.5 (C^{B10a}), 143.5 (C^{B10b}), 139.4 (C^{B4}), 138.7 (C^{B7}), 135.0 (t, J = 1.6 Hz, C^{C6}), 133.8 (t, J = 8.1 Hz, $C^{D2/D2'}$), 133.5 (t, J = 7.8 Hz, $C^{D2/D2'}$),

132.7 (t, J = 16.2 Hz, $C^{D1/D1'}$), 132.5 (t, J = 17.9 Hz, $C^{D1/D1'}$), 131.7 (C^{C3}), 130.9 ($C^{D4/D4'}$), 130.8 (C^{B6a}), 129.9 (t, J = 4.8 Hz, $C^{D3/D3'}$), 129.5 (t, J = 4.6 Hz, $C^{D3/D3'}$), 129.3 (C^{B4a}), 128.6 (C^{C5}), 128.1 (C^{B5}), 127.3 (C^{B6}), 126.2 (t, J = 2.4 Hz, C^{C4}), 125.9 (C^{B8}), 124.9 (C^{B3}), 121.4 (m, C^{C2}), 37.0 (t, J = 1.4 Hz, $C^{xantphos\text{-}bridge}$), 35.0 ($C^{Et\text{-}CH2}$), 31.4 ($C^{xantphos\text{-}Me}$), 25.7 ($C^{xantphos\text{-}Me}$), 13.1 ($C^{Et\text{-}CH3}$). ^{31}P NMR (162 MHz, $(CD_3)_2CO$, 300 K) δ/ppm: −12.7 (broad, FWHM = 340 Hz, xantphos), −144.5 (septet, J_{PF} = 708 Hz, $[PF_6]^-$). ESI MS: m/z 849.4 $[M–PF_6]^+$ (base peak, calc. 849.2). Found: C 63.51, H 4.71, N 3.14; $C_{53}H_{44}CuF_6N_2OP_3$ requires C 63.95, H 4.46, N 2.81.

[Cu(POP)(6-*t*Bubpy)][PF_6], A colourless solution of [Cu(MeCN)$_4$][PF_6] (93 mg, 0.25 mmol) and POP (134 mg, 0.25 mmol) in CH_2Cl_2 (40 mL) was stirred for 2 h. Then 6-*t*Bubpy (53 mg, 0.25 mmol) was added and the yellow solution was stirred for another 2 h. The solution was filtered and the solvent from the filtrate was removed in vacuo. The title compound [Cu(POP)(6-*t*Bubpy)][PF_6] was washed with hexane and isolated as a pale yellow powder (220 mg, 0.23 mmol, 92%). ^{1}H NMR (500 MHz, $(CD_3)_2CO$, 298 K) δ/ppm: 8.42 (d, J = 8.1 Hz, 1H, H^{A3}), 8.39 (d, J = 4.8 Hz, 1H, H^{A6}), 8.26 (dd, J = 7.9, 0.7 Hz, 1H, H^{B3}), 8.05 (t, J = 7.9 Hz, 1H, H^{B4}), 8.04 (td, J = 7.9, 1.7 Hz, 1H, H^{A4}), 7.63 (dd, J = 7.9, 0.6 Hz, 1H, H^{B5}), 7.45 (ddd, J = 8.2, 7.5, 1.7 Hz, 2H, H^{C5}), 7.41 (t, J = 7.4 Hz, 4H, H^{D4}), 7.30 (t, J = 7.1 Hz, 8H, H^{D3}), 7.23 (m, 3H, H^{A5+C6}), 7.15 (td, J = 7.5, 1.1 Hz, 2H, H^{C4}), 7.10 (broad signal, 8H, H^{D2}), 6.93 (dtd, J = 7.8, 4.0, 1.7 Hz, 2H, H^{C3}), 1.27 (s, 9H, H^{tBu}). ^{13}C NMR (126 MHz, $(CD_3)_2CO$, 298 K) δ/ppm: 170.9 (C^{B6}), 158.3 (t, J = 6.3 Hz, C^{C1}), 154.9 (C^{A2}), 154.3 (C^{B2}), 150.0 (C^{A6}), 139.9 (C^{B4}), 139.6 (C^{A4}), 135.2 (C^{C3}), 134.1 (t, J = 8.2Hz, C^{D2}), 133.3 (C^{C5}), 131.5 (t, J = 16.1 Hz, C^{D1}), 131.1 (C^{D4}), 129.8 (t, J = 4.8 Hz, C^{D3}), 126.1 (t, J = 2.4 Hz, C^{C4}), 125.9 (C^{A5}), 124.6 (t, J = 14.6 Hz, C^{C2}), 124.2 (C^{A3}), 123.2 (C^{B5}), 121.7 (C^{B3}), 120.7 (C^{C6}), 37.9 ($C(CH_3)_3$), 31.0 ($C(CH_3)_3$). ^{31}P NMR (162 MHz, $(CD_3)_2CO$, 295 K) δ/ppm: −15.1 (br, FWHM = 125 Hz, POP), −144.2 (sept, J_{PF} = 708 Hz, $[PF_6]^-$). ESI MS: m/z 813.3 $[M–PF_6]^+$ (base peak, calc. 813.2). Found: C 61.82, H 5.23, N 3.29; $C_{50}H_{44}CuF_6N_2OP_3$·0.5MeCN requires C 62.51, H 4.68, N 3.57%.

[Cu(xantphos)(6-*t*Bubpy)][PF_6], A colourless solution of xantphos (145 mg, 0.25 mmol) and 6-*t*Bubpy (53 mg, 0.25 mmol) in CH_2Cl_2 (20 mL) was added dropwise to a colourless solution of [Cu(MeCN)$_4$][PF_6] (93 mg, 0.25 mmol) in CH_2Cl_2 (20 mL). After stirring for 2h, the yellow solution was filtered and the solvent was removed in vacuo. The solid was washed with hexane, giving [Cu(POP)(6-*t*Bubpy)][PF_6] as a light yellow powder in good yield (225 mg, 0.23 mmol, 92%). ^{1}H NMR (500 MHz, $(CD_3)_2CO$, 298 K) δ/ppm: 8.47 (dt, J = 8.2, 1.0 Hz, 1H, H^{A3}), 8.29 (dd, J = 7.9, 1.0 Hz, 1H, H^{B3}), 8.24 (broad signal, 1H, H^{A6}), 8.16 (t, J = 7.9 Hz, 1H, H^{B4}), 8.11 (td, J = 8.0, 1.5 Hz, 1H, H^{A4}), 7.86 (dd, J = 7.8, 1.4 Hz, 2H, H^{C5}), 7.79 (d, J = 7.9 Hz, 1H, H^{B5}), 7.43 (m, 1H, H^{A5}), 7.38 (t, J = 7.0 Hz, 4H, H^{D4}), 7.28 (t, J = 7.7 Hz, 2H, H^{C4}), 7.21 (t, J = 7.7 Hz, 8H, H^{D3}), 7.07 (q, J = 5.5 Hz, 8H, H^{D2}), 6.72 (dtd, J = 7.6, 3.8, 1.4 Hz, 2H, H^{C3}), 1.81 (s, 6H, $Me^{xantphos}$), 1.13 (s, 9H, H^{tBu}). ^{13}C NMR (126 MHz, $(CD_3)_2CO$, 298 K) δ/ppm: 171.4 (C^{B6}), 155.4 (t, J = 6.2 Hz, C^{C1}), 154.3 (C^{B2}), 149.4 (C^{A2}), 140.2 (C^{B4}), 140.0 (C^{A4}), 134.6 (t, J = 1.8 Hz, C^{C6}), 134.1 (broad signal, C^{D1}), 131.7 (C^{C3}), 131.1 (broad signal, C^{D1+D4}), 129.8 (t, J = 4.9 Hz, C^{D3}), 128.6 (C^{C5}), 126.4 (C^{A5}), 126.2 (t, J = 2.7 Hz, C^{C4}), 124.8 (C^{A3}), 123.9 (C^{B5}), 122.4 (C^{B3}), 121.1 (t, J = 13.5 Hz, C^{C2}), 37.9 ($C(CH_3)_3$), 36.82 ($C^{xantphos\text{-}bridge}$), 36.80($Me^{xantphos}$, 31.1 ($C(CH_3)_3$). ^{31}P NMR (162 MHz, $(CD_3)_2CO$, 295 K) δ/ppm: −13.0 (br, FWHM = 133 Hz, xantphos), −144.2 (sept, J_{PF} = 709 Hz, $[PF_6]^-$). ESI MS: m/z 853.4 $[M–PF_6]^+$ (base peak, calc. 853.3). Found: C 63.30, H 5.37, N 3.17; $C_{53}H_{48}CuF_6N_2OP_3$ requires C 63.69, H 4.84, N 2.80%.

[Cu(POP)(4,5,6-Me_3bpy)][PF_6], A colourless solution of [Cu(MeCN)$_4$][PF_6] (93 mg, 0.25 mmol) and POP (134 mg, 0.25 mmol) in CH_2Cl_2 (40 mL) was stirred for 2 h. Then 4,5,6-Me_3bpy (50 mg, 0.25 mmol) was added and the yellow solution was stirred for another 2 h. The solution was filtered and the solvent from the filtrate was removed in vacuo. The yellow powder was redissolved in CH_2Cl_2 and

layered with Et_2O. This gave yellow crystals, which were powdered and washed with hexane, giving [Cu(POP)(4,5,6-Me_3bpy)][PF_6] in excellent yield (230 mg, 0.24 mmol, 96%). ^{1}H NMR (500 MHz, $(CD_3)_2CO$, 298 K) δ/ppm: 8.67 (dd, J = 5.1, 0.7 Hz, 1H, H^{A6}), 8.44 (d, J = 8.2 Hz, 1H, H^{A3}), 8.24 (s, 1H, H^{B3}), 8.03 (td, J = 8.1, 1.6 Hz, 1H, H^{A4}), 7.44–7.34 (m, 7H, $H^{A5+C5+D4}$), 7.30–7.23 (m, 8H, H^{D3}), 7.20–7.12 (8H, $H^{D2/D2'+C4+C6}$), 7.08–7.03 (m, 4H, $H^{D2/D2'}$), 6.89 (dtd, 2H, J = 7.7, 4.1, 1.6 Hz, H^{C3}), 2.49 (s, 3H, Me^{B6}), 2.31 (s, 3H, Me^{B4}), 2.15 (s, 3H, Me^{B5}). ^{13}C NMR (126 MHz, 298 K, $(CD_3)_2CO$, 298 K) δ/ppm: 158.9 (t, J = 6.0 Hz, C^{C1}), 157.9 (C^{B2}), 154.1 (t, J = 2.3 Hz, C^{A2}), 150.2 (C^{A6}), 149.7 (C^{B6}), 149.3 (t, J = 1.7 Hz, C^{B4}), 139.5 (C^{A4}), 135.0 (C^{B5}), 134.9 (C^{C3}), 134.2 (t, J = 8.3 Hz, $C^{D2/D2'}$), 133.7 (t, J = 8,2 Hz, $C^{D2/D2'}$), 133.1 (C^{C5}), 132.4–132.1 (m, $C^{D1/D1'}$), 131.0 ($C^{D4/D4'}$), 130.9 ($C^{D4/D4'}$), 129.8–129.6 (m, C^{D3}), 126.1 (C^{A5}), 126.0 (t, J = 2.2 Hz, C^{C4}), 125.2 (d, J = 13.7 Hz, $C^{C2/C2'}$), 125.1 (d, J = 13.8 Hz, $C^{C2/C2'}$), 123.0 (C^{A3}), 122.9 (C^{B3}), 121.2 (t, J = 1.9 Hz, C^{C6}), 25.8 (Me^{B6}), 20.3 (Me^{B4}), 15.4 (Me^{B5}). ^{31}P NMR (162 MHz, $(CD_3)_2CO$, 295 K) δ/ppm: −12.9 (br, FWHM = 252 Hz, POP), −144.2 (sept, J_{PF} = 708 Hz, $[PF_6]^-$). ESI MS: m/z 799.2 $[M–PF_6]^+$ (base peak, calc. 799.2). Found: C 62.13, H 4.78, N 2.93; $C_{49}H_{42}CuF_6N_2OP_3$ requires C 62.26, H 4.48, N 2.96%.

[Cu(xantphos)(4,5,6-Me_3bpy)][PF_6], A colourless solution of xantphos (111 mg, 0.19 mmol) and 4,5,6-Me_3bpy (38 mg, 0.19 mmol) in CH_2Cl_2 (20 mL) was added dropwise to a colourless solution of [$Cu(MeCN)_4$][PF_6] (71 mg, 0.19 mmol) in H_2Cl_2 (20 mL). After stirring for 2h, the yellow solution was filtered and the solvent was removed in vacuo. The yellow powder was redissolved in CH_2Cl_2 and layered with Et_2O. This yielded yellow crystals, which were powdered and washed with hexane, giving [Cu(xantphos)(4,5,6-Me_3bpy)][PF_6] in excellent yield (182 mg, 0.18 mmol, 95 %). ^{1}H NMR (500 MHz, $(CD_3)_2CO$, 298 K) δ/ppm: 8.49 (d, J = 8.1 Hz, 1H, H^{A3}), 8.40 (d, J = 4.7 Hz, 1H, H^{A6}), 8.29 (s, 1H, H^{B3}), 8.05 (t, J = 7.8 Hz, 1H, H^{A4}), 7.85 (d, J = 7.7 Hz, 2H, H^{C5}), 7.43–7.31 (m, 5H, H^{A5+D4}), 7.28 (t, J = 7.8 Hz, 2H, H^{C4}), 7.24 (t, J = 7.5 Hz, 4H, $H^{D3/D3'}$), 7.19–7.12 (m, 8H, $H^{D2/D2'+D3/D3'}$), 6.98–6.93 (m, 4H, $H^{D2/D2'}$), 6.67–6.63 (m, 2H, H^{C3}), 2.51 (s, 3H, Me^{B6}), 2.18 (s, 3H, Me^{B4}), 2.13 (s, 3H, Me^{B5}), 1.88 (s, 3H, $Me^{xantphos}$), 1.71 (s, 3H, $Me^{xantphos}$). ^{13}C NMR (126 MHz, 298 K, $(CD_3)_2CO$, 298 K) δ/ppm: 157.2 (C^{B2}), 155.8 (t, J = 6.3 Hz, C^{C1}), 154.0 (t, J = 2.3 Hz, C^{A2}), 150.1 (C^{B6}), 149.6 (C^{A6}), 149.1 (t, J = 1.7 Hz, C^{B4}), 139.7 (C^{A4}), 135.1 (C^{C6}), 135.0 (t, J = 1.7 Hz, C^{B5}), 133.9 (t, J = 8.0 Hz, $C^{D2/D2'}$), 133.5 (t, J = 7.8 Hz, $C^{D2/D2'}$), 132.7 (q, J = 17.7, 16.8 Hz, $C^{D1/D1'}$), 131.5 (C^{C3}), 131.0 ($C^{D4/D4'}$), 130.9 ($C^{D4/D4'}$), 129.8 (t, J = 4.7 Hz, $C^{D3/D3'}$), 129.7 (t, J = 4.7 Hz, $C^{D3/D3'}$), 128.4 (C^{C5}), 126.4 (C^{A5}), 126.2 (t, J = 2.4 Hz, C^{C4}), 123.2 (C^{A3}), 123.0 (C^{B3}), 121.5 (d, J = 12.8 Hz, $C^{C2/C2'}$), 121.4 (d, J = 12.8 Hz, $C^{C2/C2'}$), 30.0 ($Me^{xantphos}$), 26.8 ($Me^{xantphos}$), 25.5 (Me^{B6}), 20.4(Me^{B4}), 15.4 (Me^{B5}). ^{31}P NMR (162 MHz, $(CD_3)_2CO$, 295 K) δ/ppm: −13.1 (br, FWHM = 375 Hz, xantphos), −144.2 (sept, J_{PF} = 708 Hz, $[PF_6]^-$). ESI MS: m/z 839.2 $[M–PF_6]^+$ (base peak, calc. 839.2). Found: C 63.00, H 4.71, N 2.84; $C_{52}H_{46}CuF_6N_2OP_3$ requires C 63.38, H 4.71, N 2.84%.

1.3. Crystallography

Single crystal X-ray diffraction data were collected on a Bruker Kappa Apex2 diffractometer with data reduction, solution and refinement using the programs APEX[7] and CRYSTALS.[8] Structural analysis was carried out using Mercury v.4.0.0.[9,10]

[Cu(POP)(5,5'-Me_2bpy)][PF_6], $C_{48}H_{40}CuF_6N_2OP_3$, M = 931.31, yellow block, monoclinic, space group $P2_1/n$, a = 18.554(2), b = 11.4743(12), c = 22.167(2) Å, β = 113.880(4)°, U = 4315.1(8) Å^3, Z = 4, D_c = 1.433 Mg m^{-3}, μ(Cu-Kα) = 2.326 mm^{-1}, T = 123 K. Total 43751 reflections, 7916 unique, R_{int} = 0.031. Refinement of 7850 reflections (550 parameters) with $I > 2\sigma(I)$ converged at final R_1 = 0.0284 (R_1 all data = 0.0287), wR_2 = 0.0639 (wR_2 all data = 0.0640), gof = 0.9127. CCDC 1978436.

[Cu(xantphos)(5,5'-Me_2bpy)][PF_6], $C_{51}H_{44}CuF_6N_2OP_3$, M = 971.38, yellow block, monoclinic, space group $P2_1$, a = 10.1954(10), b = 21.104(2), c = 10.7666(10) Å, β = 102.835(3)°, U = 2258.7(4) Å^3, Z = 2,

D_c = 1.428 Mg m^{-3}, μ(Cu-Kα) = 2.246 mm^{-1}, T = 123 K. Total 18116 reflections, 7503 unique, R_{int} = 0.024. Refinement of 7456 reflections (578 parameters) with $I > 2\sigma(I)$ converged at final R_1 = 0.0195 (R_1 all data = 0.0195), wR_2 = 0.0220 (wR_2 all data = 0.0220), gof = 1.0919. CCDC 1978439.

[Cu(POP)(6-*t*Bubpy)][PF_6], $C_{50}H_{44}CuF_6N_2OP_3$, M = 959.37, yellow plate, monoclinic, space group $P2_1/c$, a = 12.3597(8), b = 16.6878(11), c = 21.4238(14) Å, β = 99.561(2)°, U = 4357.4(5) Å^3, Z = 4, D_c = 1.462 Mg m^{-3}, μ(Cu-Kα) = 2.320 mm^{-1}, T = 123 K. Total 55483 reflections, 7969 unique, R_{int} = 0.031. Refinement of 7917 reflections (568 parameters) with $I > 2\sigma(I)$ converged at final R_1 = 0.0479 (R_1 all data = 0.0480), wR_2 = 0.0476 (wR_2 all data = 0.0477), gof = 1.0970. CCDC 1978441.

[Cu(POP)(4,5,6-Me_3bpy)][PF_6]·1.5Et_2O, $C_{55}H_{57}CuF_6N_2O_{2.5}P_3$ or $C_{49}H_{42}CuF_6N_2OP_3$·1.5$C_4H_{10}O$, M = 1056.52, green block, triclinic, space group $P\bar{1}$, a = 9.7384(7), b = 14.1543(10), c = 18.9271(13) Å, α = 74.958(2), β = 84.595(2), γ = 87.789(3)°, U = 2508.1(3) Å^3, Z = 2, D_c = 1.40 Mg m^{-3}, μ(Cu-Kα) = 2.088 mm^{-1}, T = 130 K. Total 30758 reflections, 9047 unique, R_{int} = 0.023. Refinement of 8371 reflections (559 parameters) with $I > 2\sigma(I)$ converged at final R_1 = 0.0490 (R_1 all data = 0.0521), wR_2 = 0.1441 (wR_2 all data = 0.1501), gof = 0.9723. CCDC 1978440.

[Cu(xantphos)(4,5,6-Me_3bpy)][PF_6]·2.33CH_2Cl_2, $C_{54.33}H_{50.66}Cl_{4.66}CuF_6N_2OP_3$ or $C_{52}H_{46}CuF_6N_2OP_3$+2.33(CH_2CL_2), M = 1183.30, yellow block, triclinic, space group $P\bar{1}$, a = 11.8055(3), b = 15.0529(4), c = 18.6132(5) Å, α = 113.589(2), β = 92.960(2), γ = 108.444(2)°, U = 2814.51(15) Å^3, Z = 2, D_c = 1.40 Mg m^{-3}, μ(Cu-Kα) = 4.312 mm^{-1}, T = 130 K. Total 99434 reflections, 10831 unique, R_{int} = 0.0573. Refinement of 6531 reflections (586 parameters) with $I > 2\sigma(I)$ converged at final R_1 = 0.0987 (R_1 all data = 0.1253), wR_2 = 0.2929 (wR_2 all data = 0.3222), gof = 1.0878. CCDC 1978438.

[Cu(POP)(2-Etphen)][PF_6], $C_{50}H_{40}CuF_6N_2OP_3$, M = 955.33, yellow block, triclinic, space group $P\bar{1}$, a = 10.1640(8), b = 13.9335(11), c = 18.7219(14) Å, α = 102.552(2), β = 97.085(2), γ = 107.584(2)°, U = 2415.7(3) Å^3, Z = 2, D_c = 1.43 Mg m^{-3}, μ(Cu-Kα) = 3.133 mm^{-1}, T = 123 K. Total 32433 reflections, 8856 unique, R_{int} = 0.026. Refinement of 8704 reflections (568 parameters) with $I > 2\sigma(I)$ converged at final R_1 = 0.0340 (R_1 all data = 0.0344), wR_2 = 0.0808 (wR_2 all data = 0.0808), gof = 0.9218. CCDC 1978437.

[Cu(xantphos)(2-Etphen)][PF_6], $C_{53}H_{44}CuF_6N_2OP_3$, M = 995.40, yellow block, monoclinic, space group $P2_1/n$, a = 10.5631(8), b = 21.3906(16), c = 20.2696(15) Å, β = 93.185(3)°, U = 4572.9(6)Å^3, Z = 4, D_c = 1.446 Mg m^{-3}, μ(Cu-Kα) = 2.234 mm^{-1}, T = 123 K. Total 31841 reflections, 8090 unique, R_{int} = 0.029. Refinement of 7552 reflections (595 parameters) with $I > 2\sigma(I)$ converged at final R_1 = 0.0444 (R_1 all data = 0.0471), wR_2 = 0.1010 (wR_2 all data = 0.1019), gof = 0.8993. CCDC 1978442.

1.4. Computational details

The complexes of interest were theoretically investigated by density functional theory (DFT) calculations. The [Cu(P^P)(N^N)]$^+$ cations ((P^P) = xantphos, POP; (N^N) = 5,5'-Me_2bpy, 4,5,6-Me_3bpy, 6-*t*Bubpy and 2-Etphen) were studied using the A.03 revision of Gaussian 16.[11] The geometries of the singlet ground electronic state (S_0) and the lowest-energy triplet excited state (T_1) were optimized for each system without the imposition of any symmetry restriction. The B3LYP exchange-correlation functional[12,13] was employed, the unrestricted UB3LYP approximation being used for the calculation of the triplet states. To better describe the intramolecular non-covalent interactions, which are expected to influence significantly the molecular geometry of the complexes, the Grimme's D3 dispersion term with Becke–Johnson damping was added to the B3LYP functional (B3LYP-D3).[14,15] Regarding the basis set, the "double-ζ" quality def2-SVP basis set was employed for the C, H, P, N and O atoms and the "triple-ζ" quality def2-TZVP basis set was used for Cu atoms.[16,17]

The time-dependent DFT (TD-DFT) approach[18,19,20] was employed to calculate the lowest-lying excited states of each cation (five singlets and five triplets), at the minimum-energy geometry computed for S_0. The solvent was considered via the self-consistent reaction field (SCRF) theory and using the polarized continuum model (PCM) approach.[21,22,23] The solvent used in all calculations was CH_2Cl_2.

1.5. Device fabrication and characterization

LECs were prepared on top of patterned indium tin oxide (ITO, 15 Ω sq^{-1}) coated glass substrates previously cleaned by chemical and UV-ozone methods. Prior to the deposition of the emitting layers, 80 nm thick films of poly-(3,4-ethylenedioxythiophene):poly(styrenesulfonate) (PEDOT:PSS, CLEVIOS™ P VP AI 4083, Heraeus) were coated in order to flatten the ITO electrode and to increase its work function. The emitting layer (approximately 100 nm thick) was prepared by spin-coating a dichloromethane solution of the emitting compound with the addition of the ionic liquid 1-ethyl-3-methylimidazolium hexafluorophosphate [EMIM][PF_6] (>98.5%, Sigma-Aldrich), in a 4:1 molar ratio. The devices were then transferred to an inert atmosphere glovebox (<0.1 ppm O_2 and H_2O), where the aluminium cathode (100 nm) was thermally deposited in high vacuum using an Edwards Auto500 chamber integrated in the glovebox. The thickness of all films was determined with an Ambios XP-1 profilometer. The active area of the devices was 6.5 mm^2. LECs were not encapsulated and were characterized inside the glovebox at room temperature. The device lifetime was measured by applying a pulsed current and monitoring the voltage and luminance *vs* time by a true colour sensor MAZeT (MTCSiCT Sensor) with a Botest OLT OLED Lifetime-Test System. The electroluminescence (EL) spectra were measured using an Avantes AvaSpec-2048 Fiber Optic Spectrometer during device lifetime measurement.

2. Data

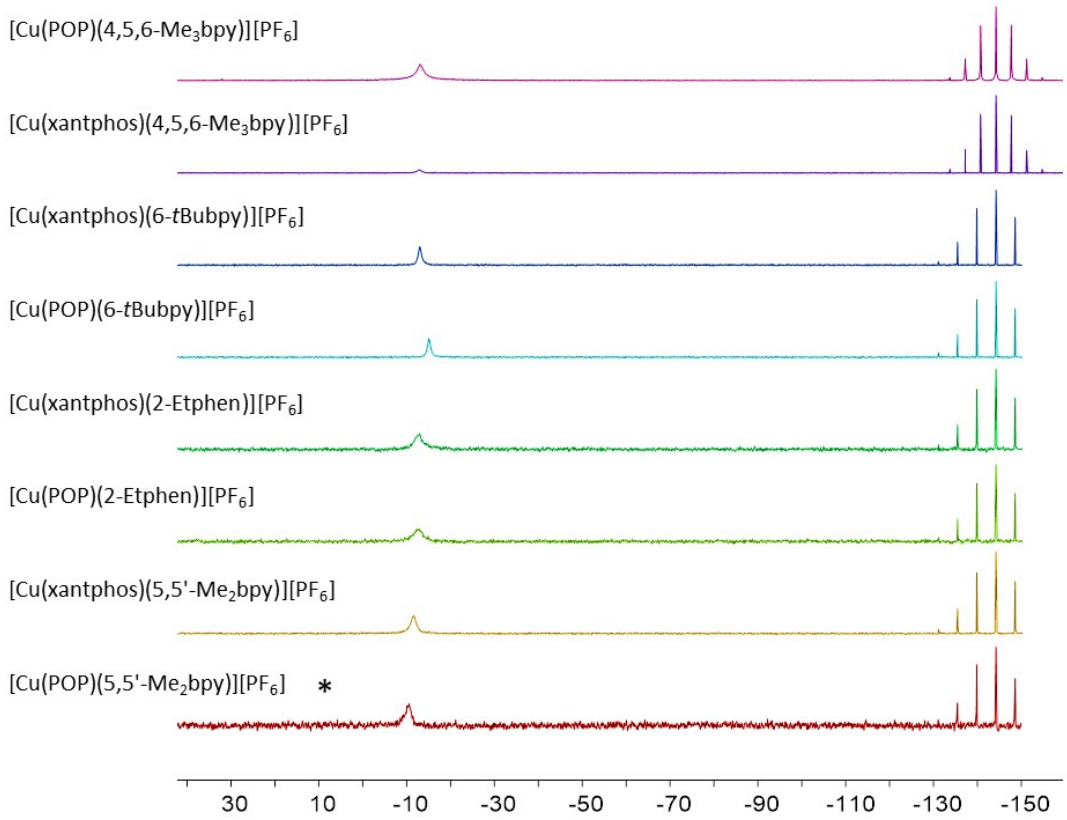

Fig. S1 ^{31}P NMR spectra of the [Cu(P^P)(N^N)][PF_6] complexes in acetone-d_6 or CD_2Cl_2 (marked with an asterisk).

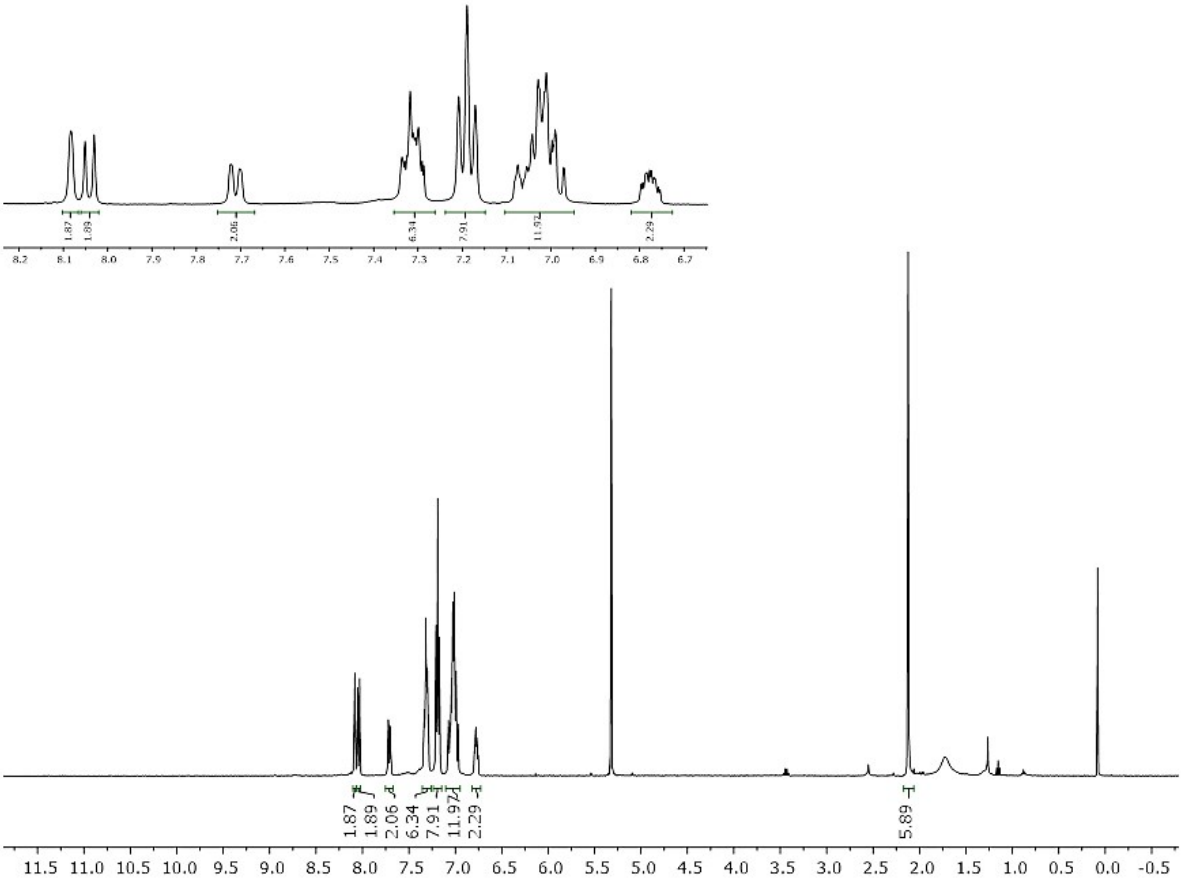

Fig. S2 ^{1}H NMR spectra of [Cu(POP)(5,5'-Me_2bpy)][PF_6] in acetone-d_6, 300 K, 400 MHz.

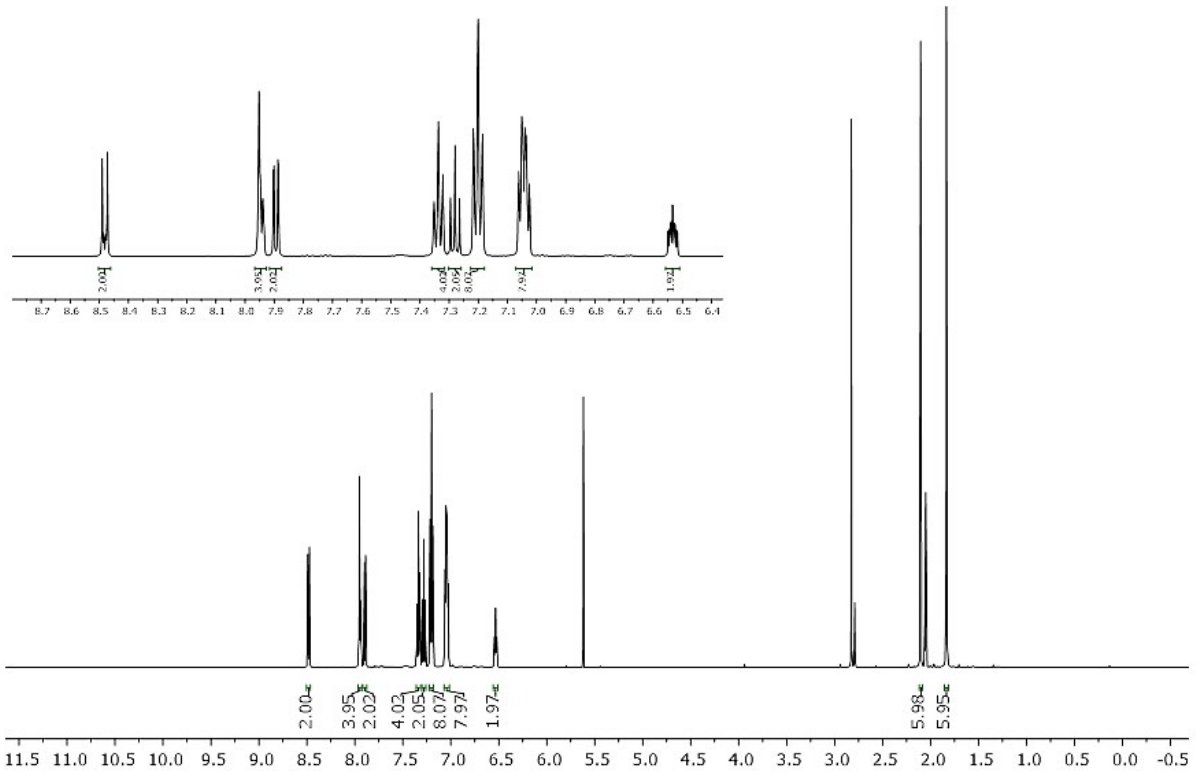

Fig. S3 ^{1}H NMR spectra of [Cu(xantphos)(5,5'-Me_2bpy)][PF_6] in acetone-d^6, 298 K, 500 MHz.

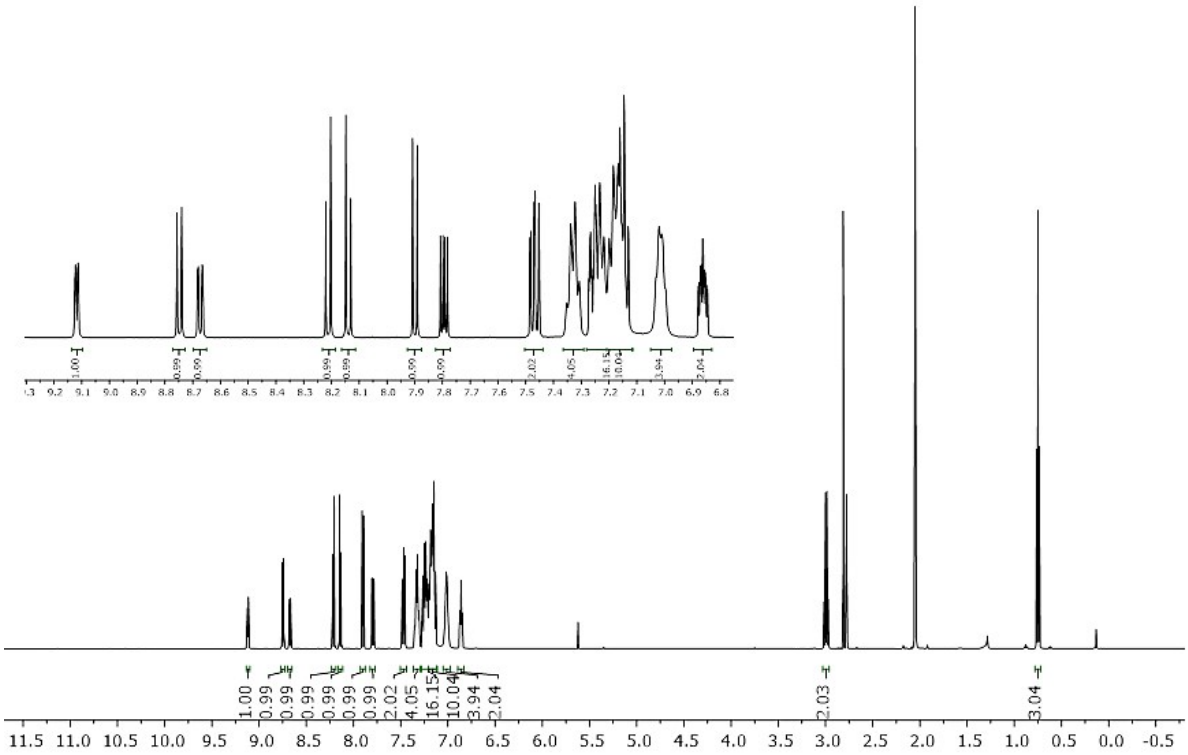

Fig. S4 ^{1}H NMR spectra of [Cu(POP)(2-Etphen)][PF_6] in acetone-d_6, 298 K, 500 MHz.

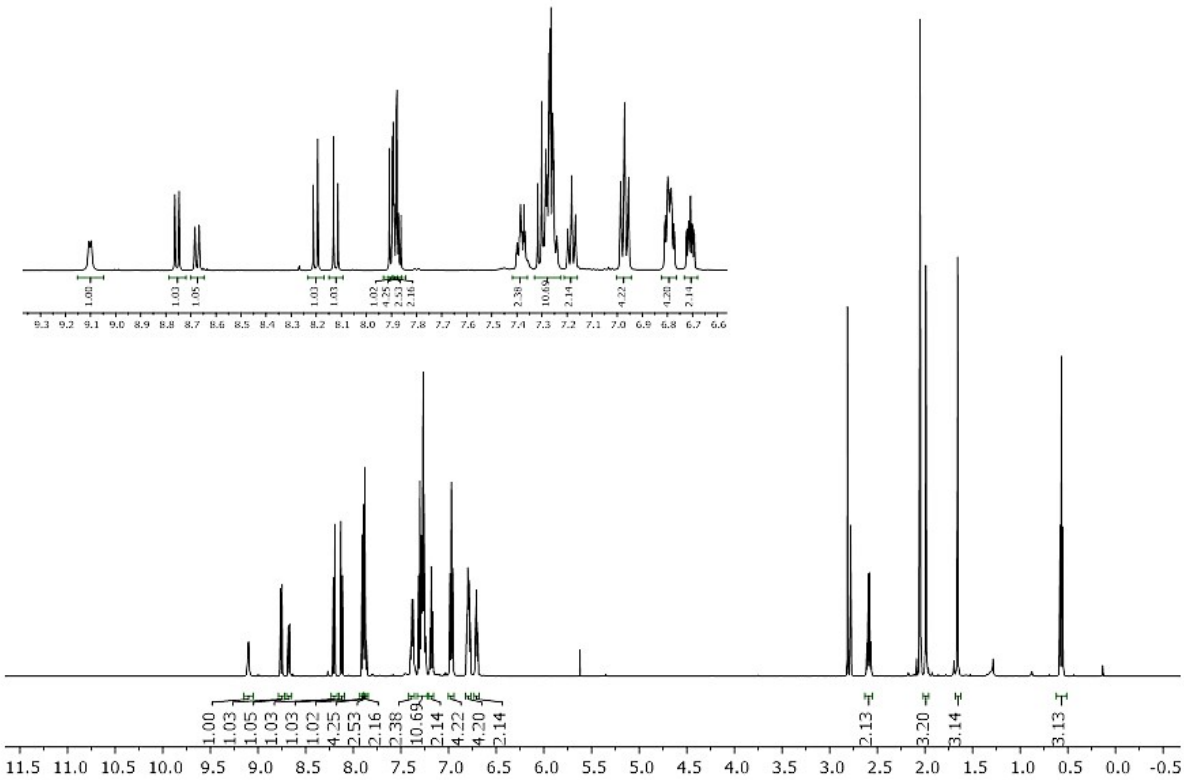

Fig. S5 ^{1}H NMR spectra of [Cu(xantphos)(2-Etphen)][PF_6] in acetone-d_6, 298 K, 500 MHz.

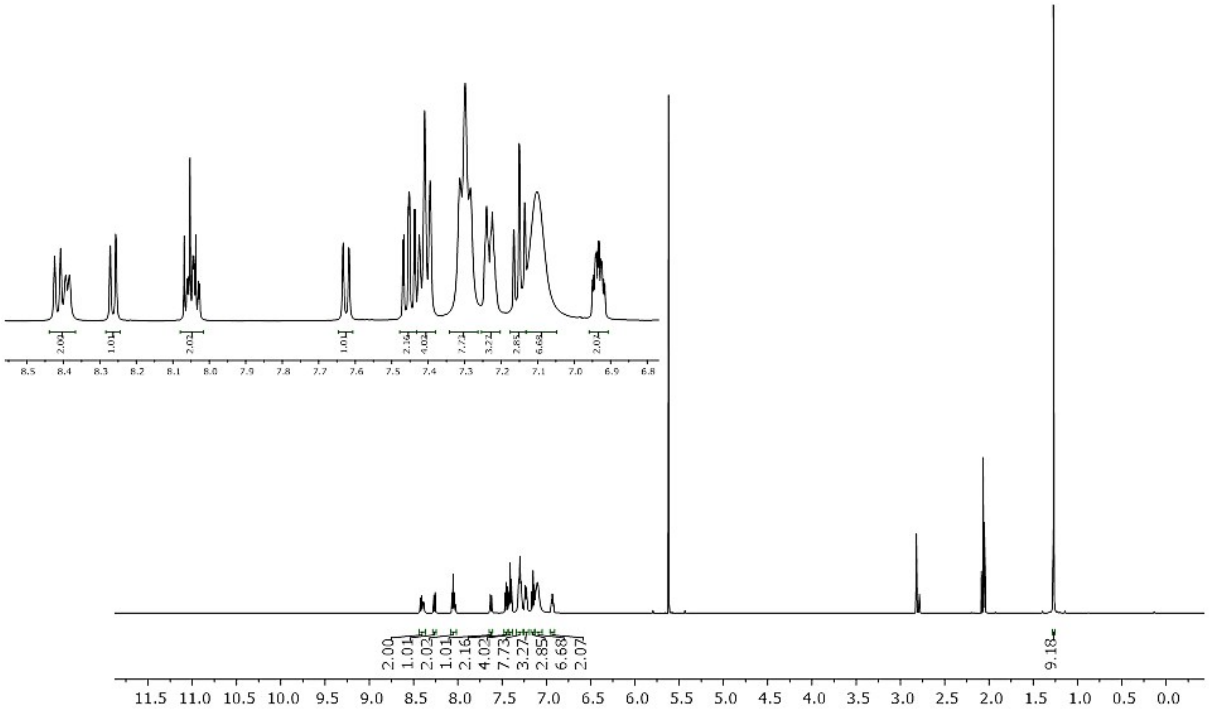

Fig. S6 ^{1}H NMR spectra of [Cu(POP)(6-*t*Bubpy)][PF_6] in acetone-d_6, 298 K, 500 MHz.

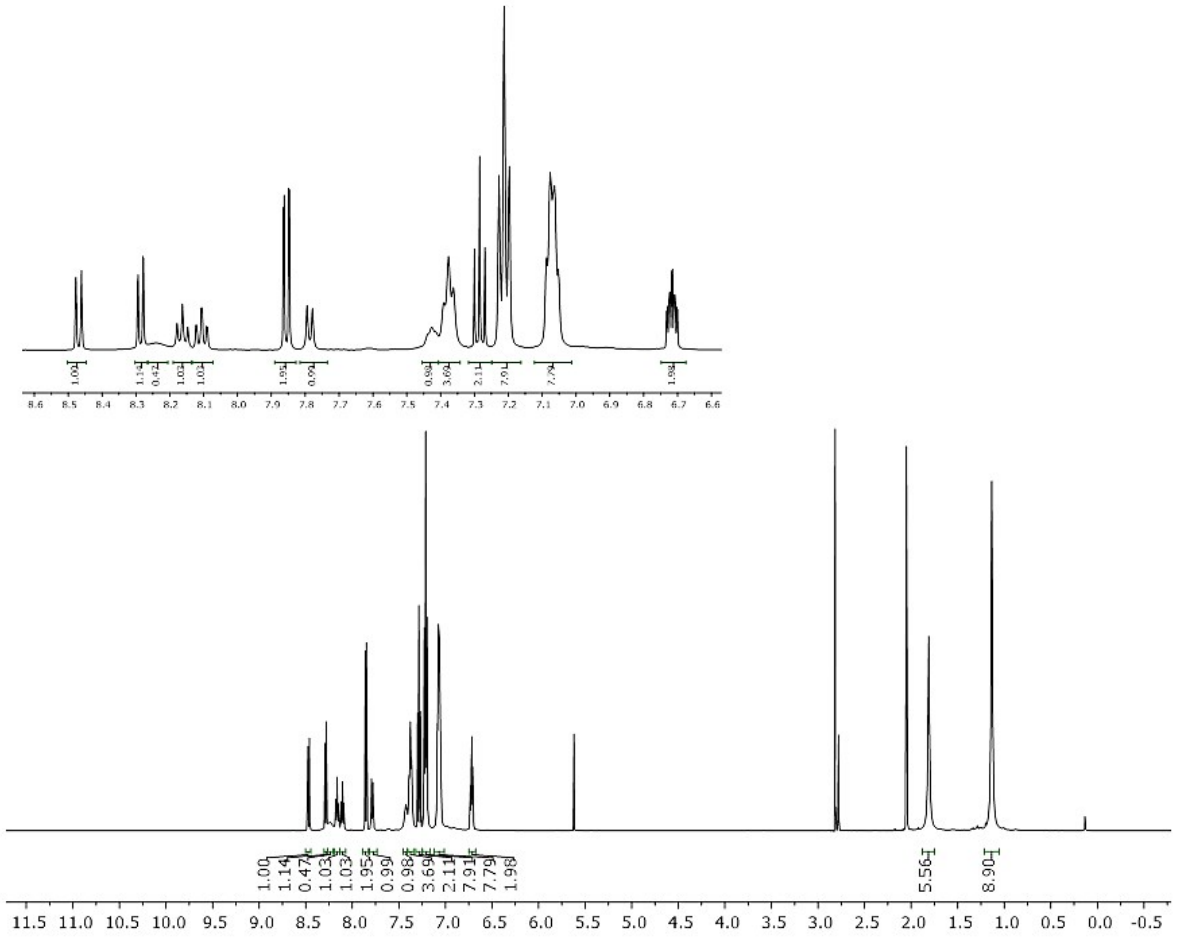

Fig. S7 ^{1}H NMR spectra of [Cu(xantphos)(6-*t*Bubpy)][PF_6] in acetone-d_6, 298 K, 500 MHz.

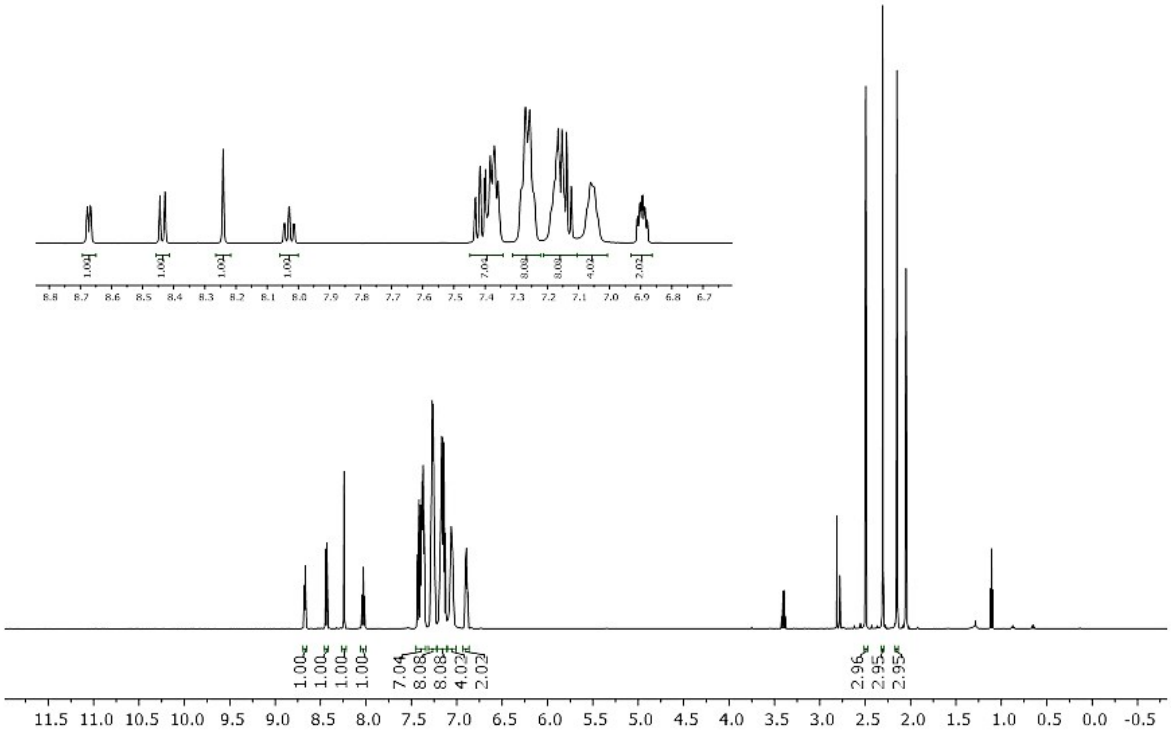

Fig. S8 ^{1}H NMR spectra of [Cu(POP)(4,5,6-Me$_3$bpy)][PF$_6$] in acetone-d_6, 298 K, 500 MHz.

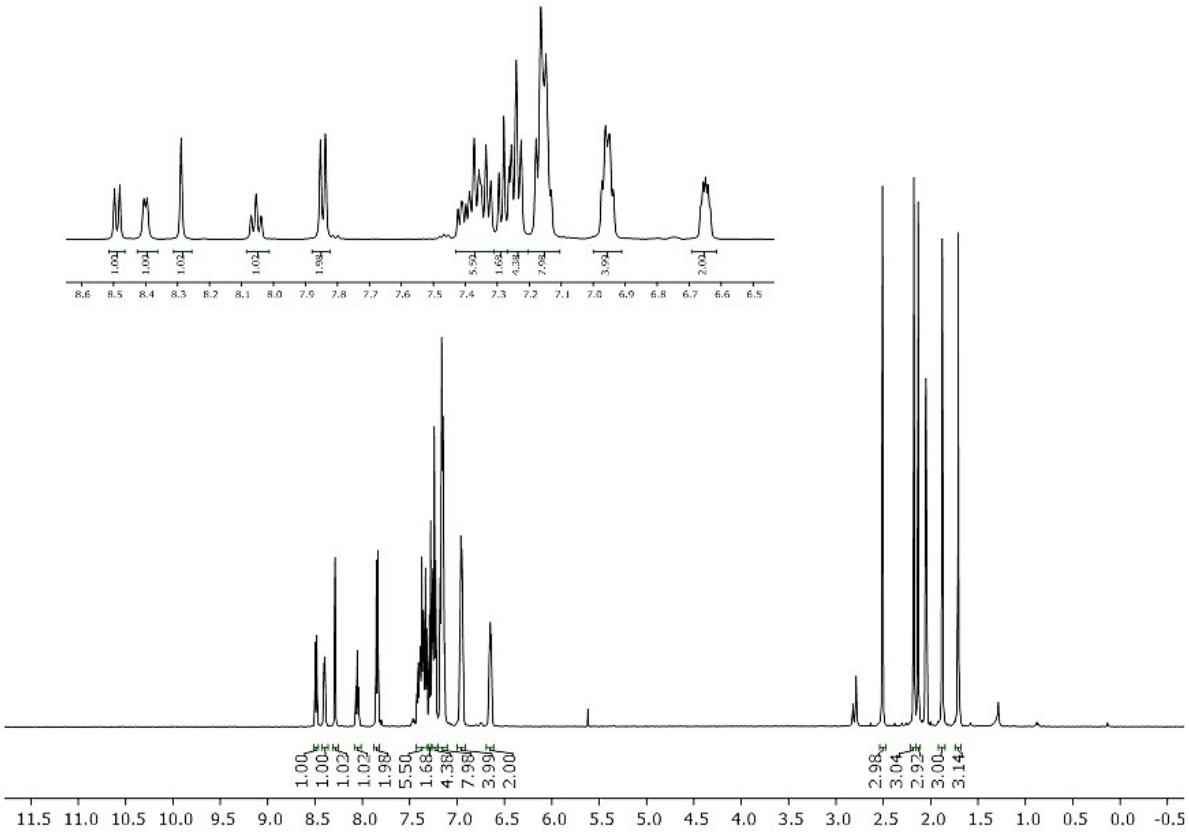

Fig. S9 ^{1}H NMR spectra of [Cu(xantphos)(4,5,6-Me$_3$bpy)][PF$_6$] in acetone-d_6, 298 K, 500 MHz.

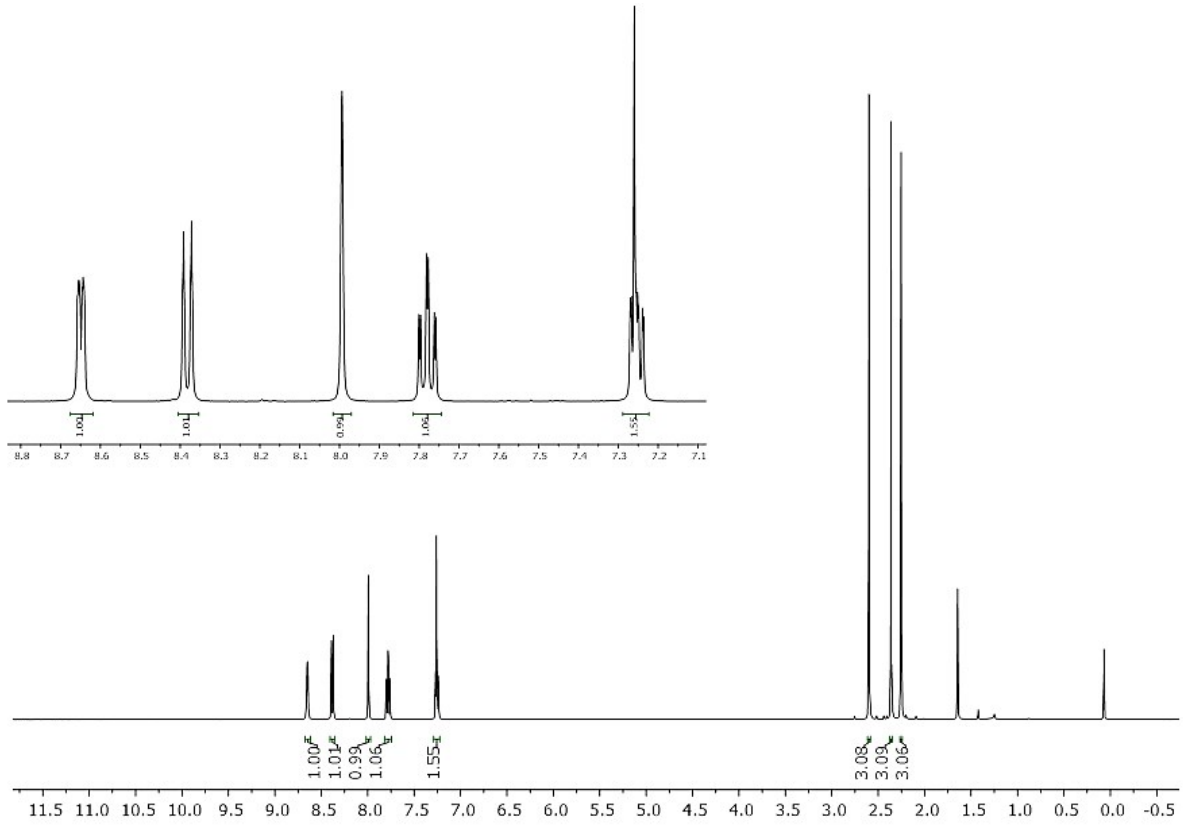

Fig. S10 ^{1}H NMR spectra of 4,5,6-Me_3bpy in $CDCl_3$, 298 K, 500 MHz.

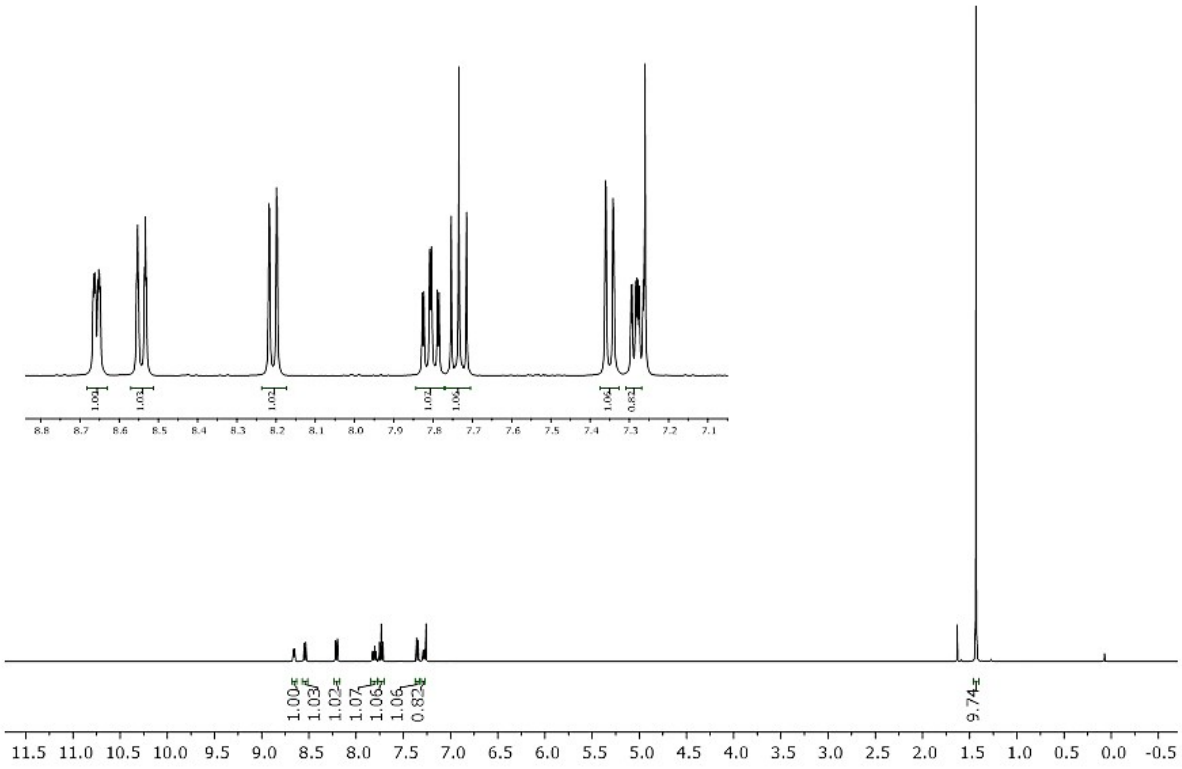

Fig. S11 ^{1}H NMR spectra of 6-*t*Bubpy in $CDCl_3$, 298 K, 500 MHz.

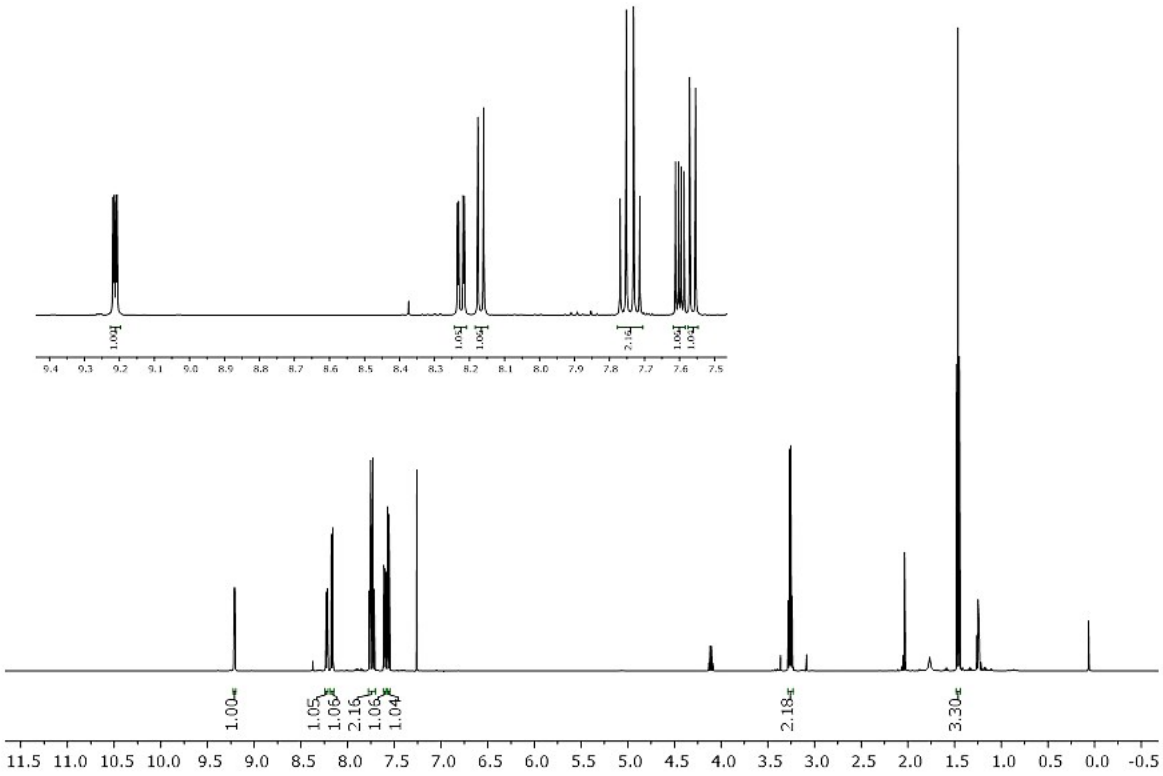

Fig. S12 ^{1}H NMR spectra of 2-Etphen in $CDCl_3$, 298 K, 500 MHz.

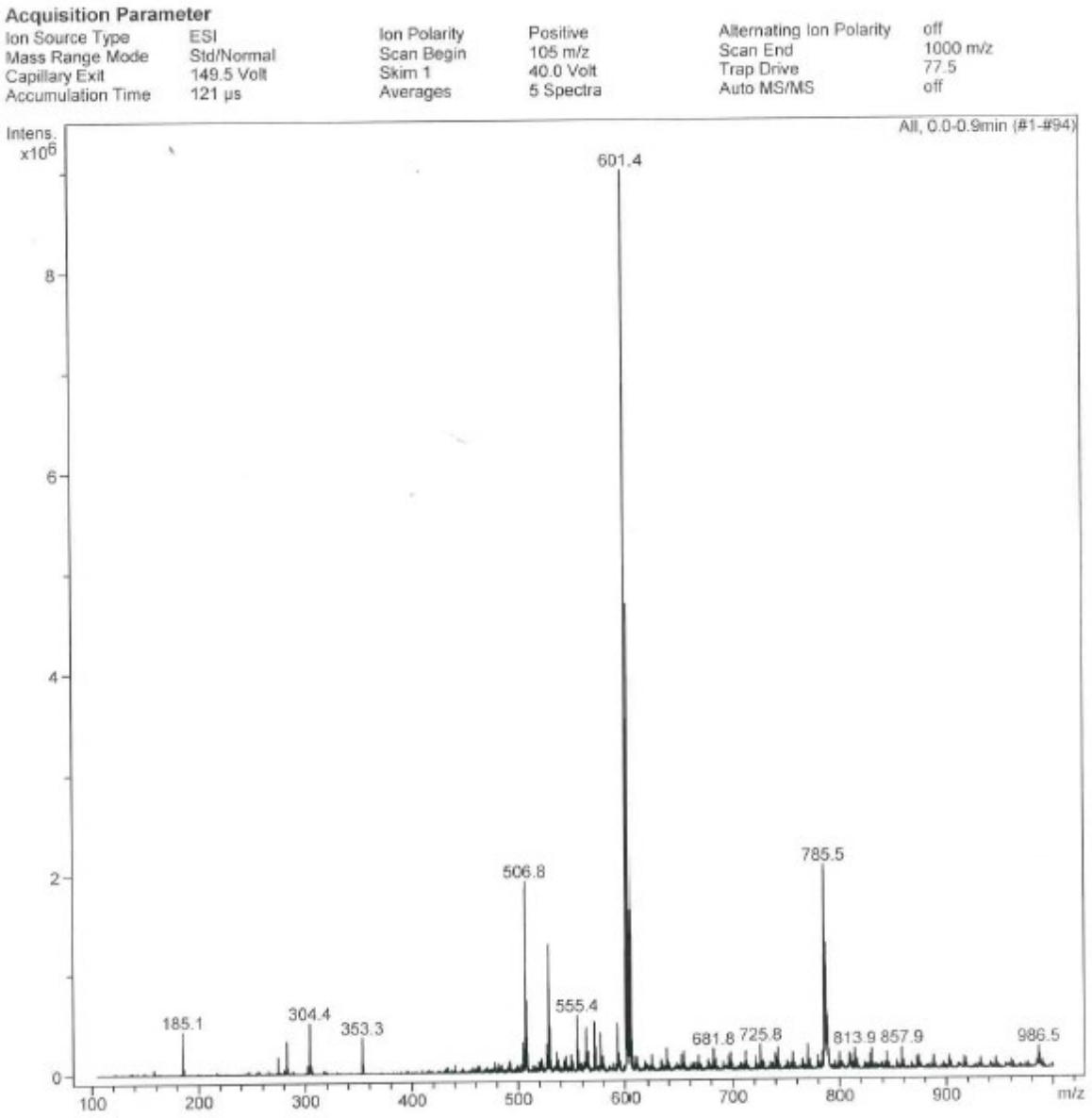

Fig. S13 ESI-MS of [Cu(POP)(5,5'-Me_2bpy)][PF_6].

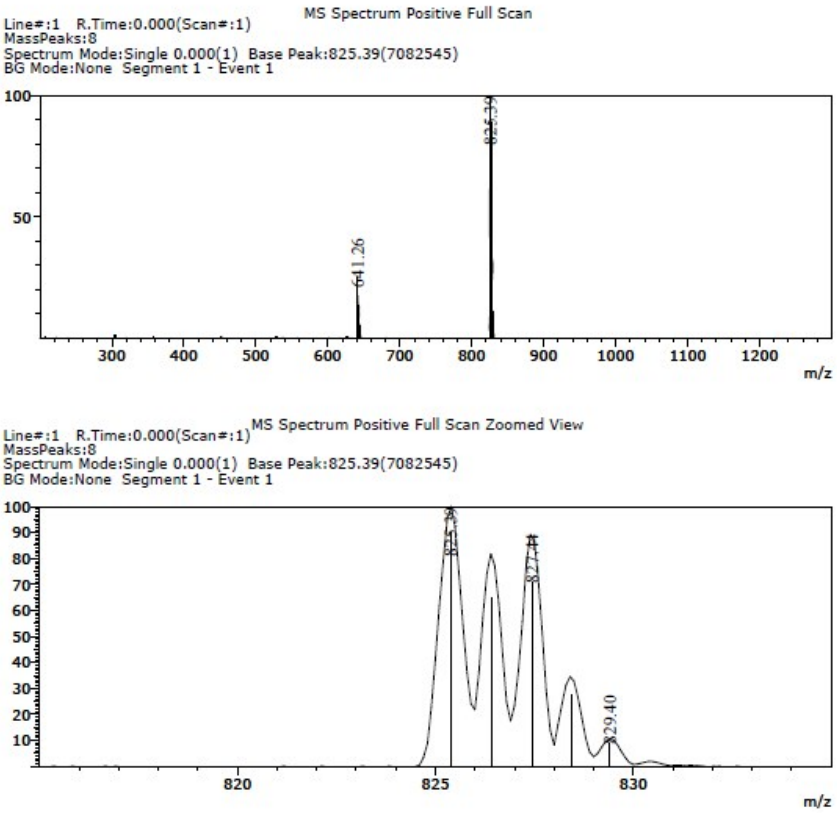

Fig. S14 ESI-MS of [Cu(xantphos)(5,5'-Me_2bpy)][PF_6].

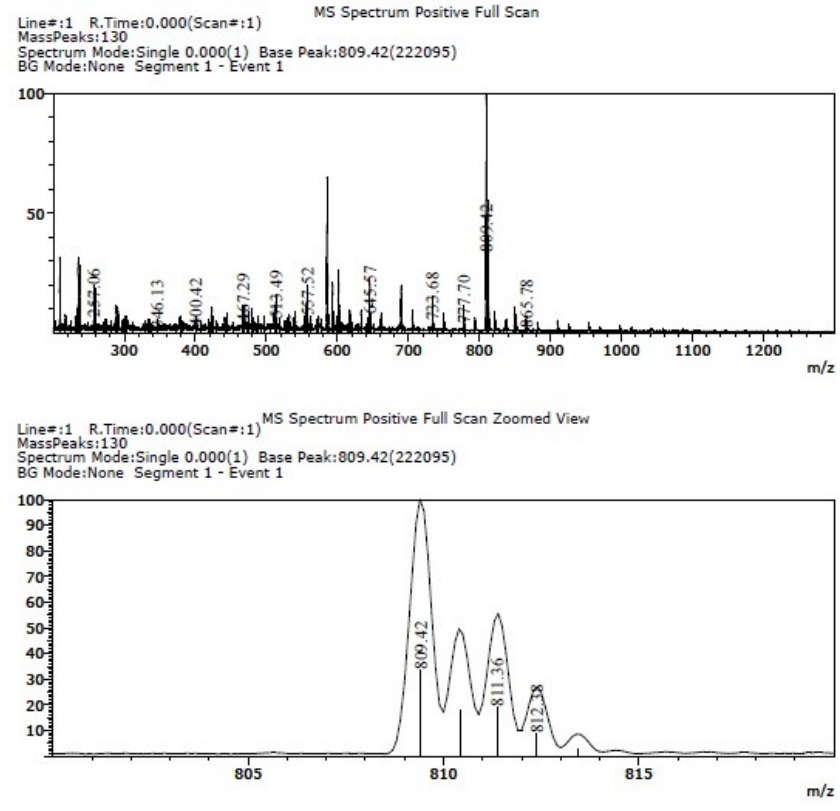

Fig. S15 ESI-MS of [Cu(POP)(2-Etphen)][PF_6].

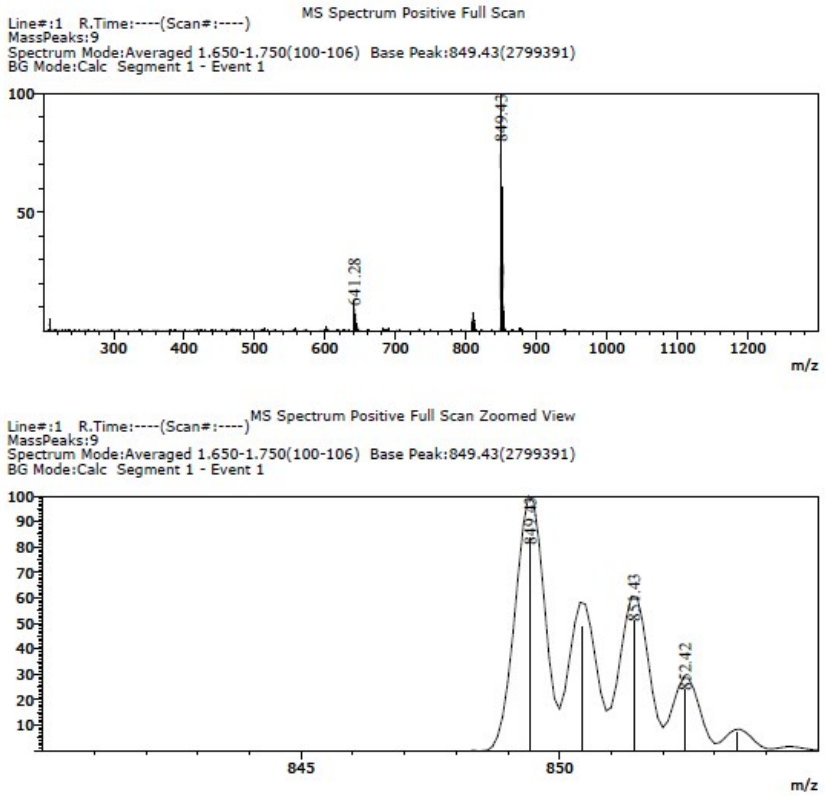

Fig. S16 ESI-MS of [Cu(xantphos)(2-Etphen)][PF_6].

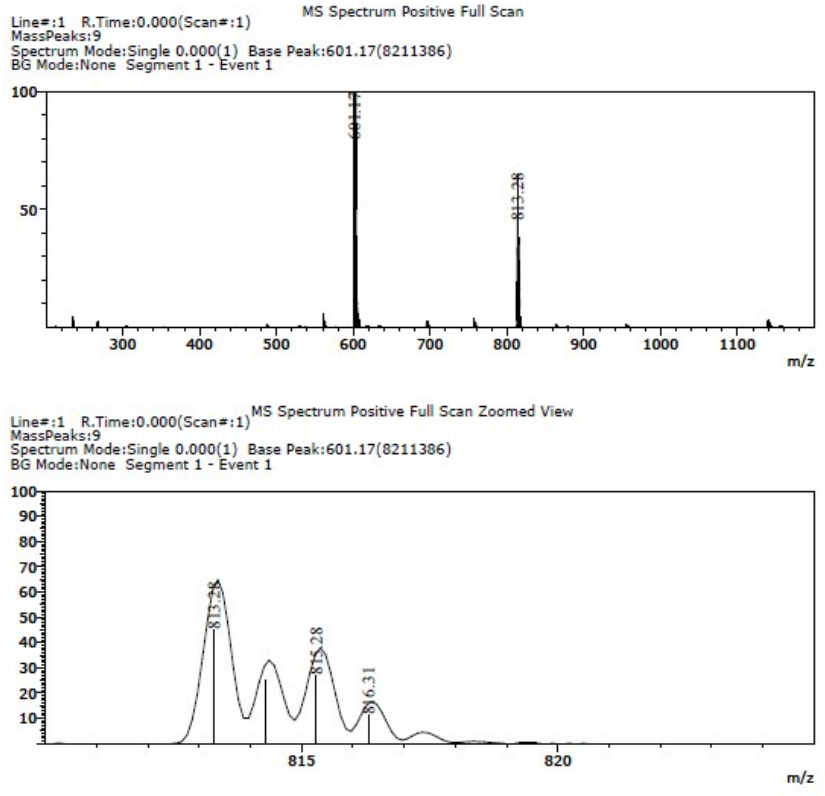

Fig. S17 ESI-MS of [Cu(POP)(6-*t*Bubpy)][PF_6].

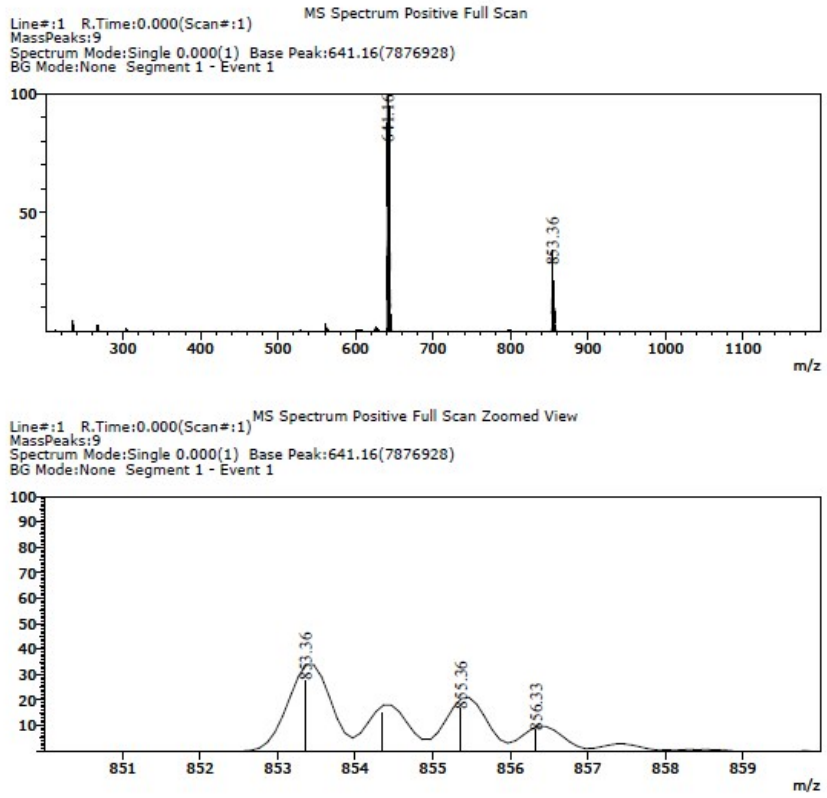

Fig. S18 ESI-MS of [Cu(xantphos)(6-*t*Bubpy)][PF_6].

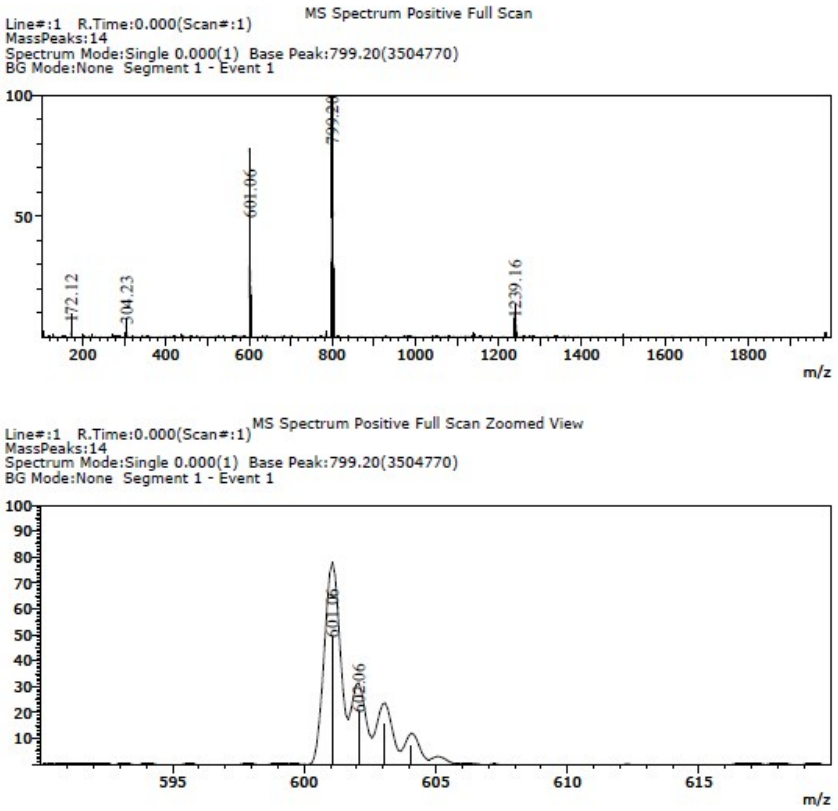

Fig. S19 ESI-MS of [Cu(POP)(4,5,6-Me_3bpy)][PF_6].

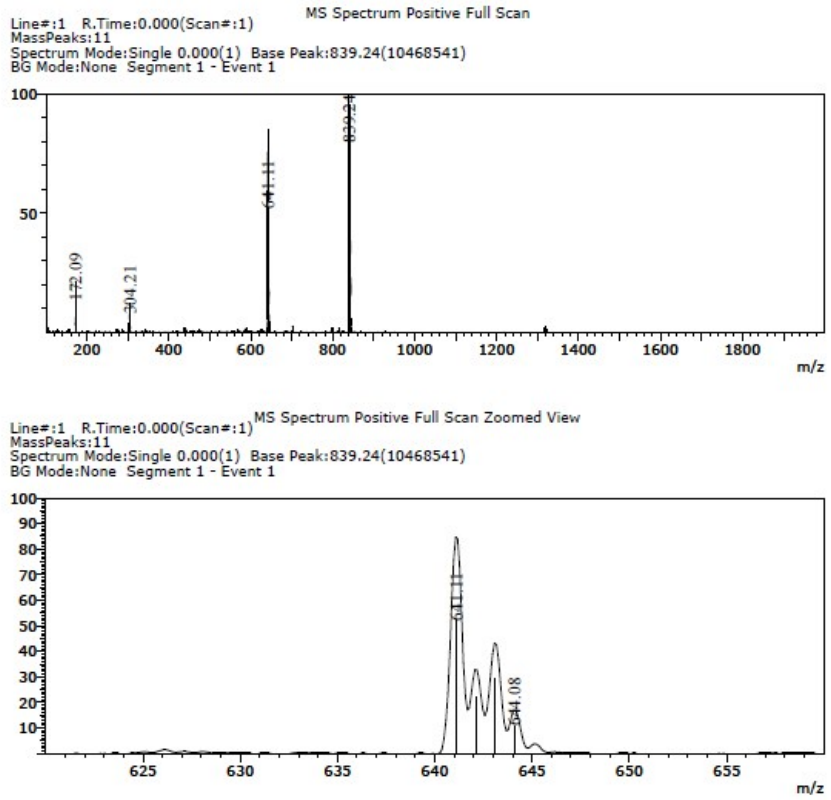

Fig. S20 ESI-MS of [Cu(xantphos)(4,5,6-Me_3bpy)][PF_6].

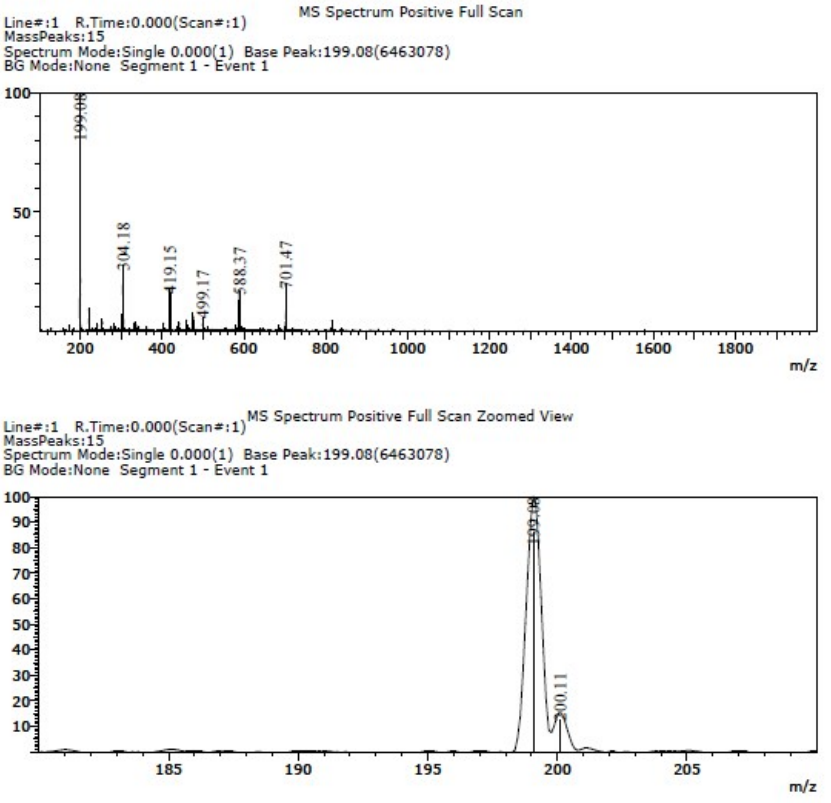

Fig. S21 ESI-MS of 4,5,6-Me_3bpy.

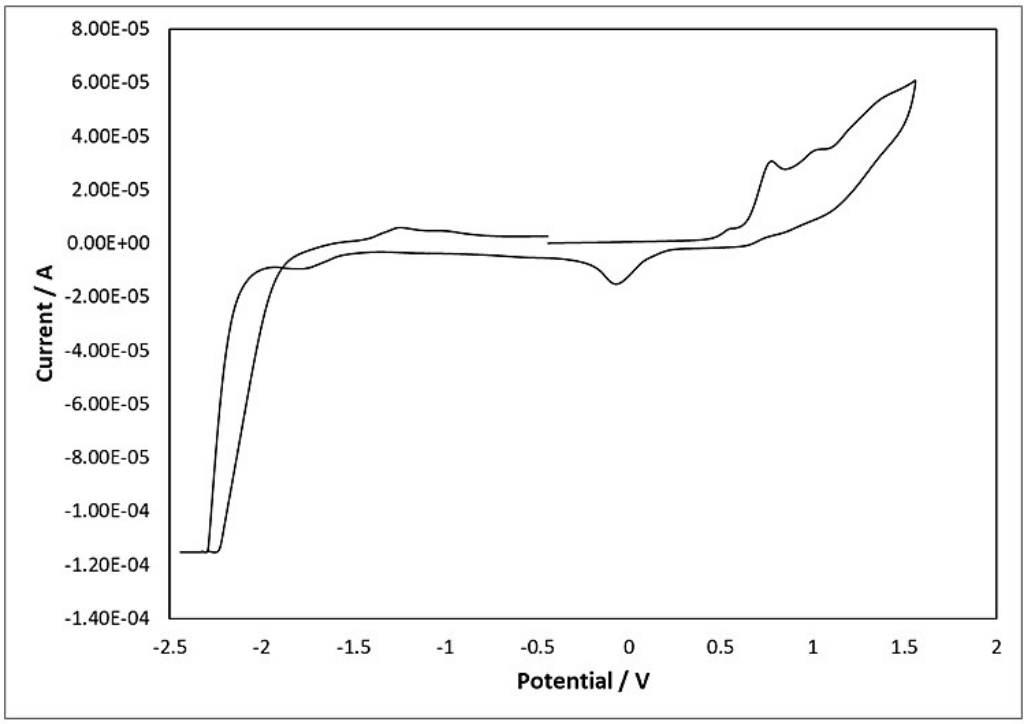

Fig. S22 Cyclic voltammogram of a CH_2Cl_2 solution of [Cu(POP)(5,5'-Me_2bpy)][PF_6] (vs. Fc^+/Fc, [$n$$Bu_4$N][$PF_6$] supporting electrolyte, scan rate = 0.1 V s^{-1}).

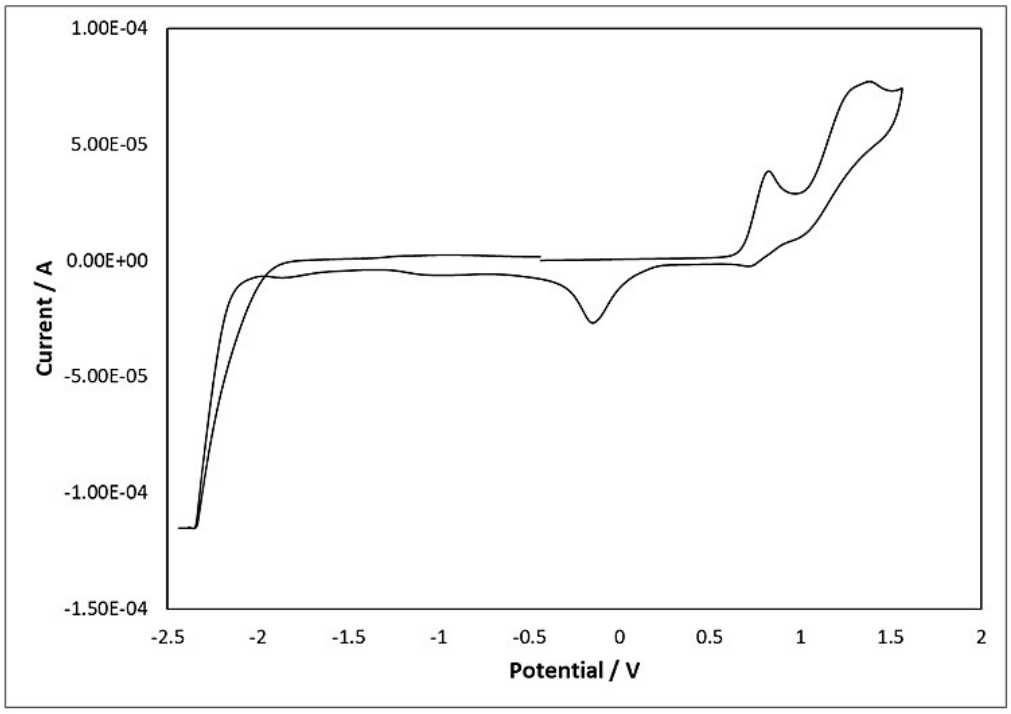

Fig. S23 Cyclic voltammogram of a CH_2Cl_2 solution of [Cu(xantphos)(5,5'-Me_2bpy)][PF_6] (vs. Fc^+/Fc, [$n$$Bu_4$N][$PF_6$] supporting electrolyte, scan rate = 0.1 V s^{-1}).

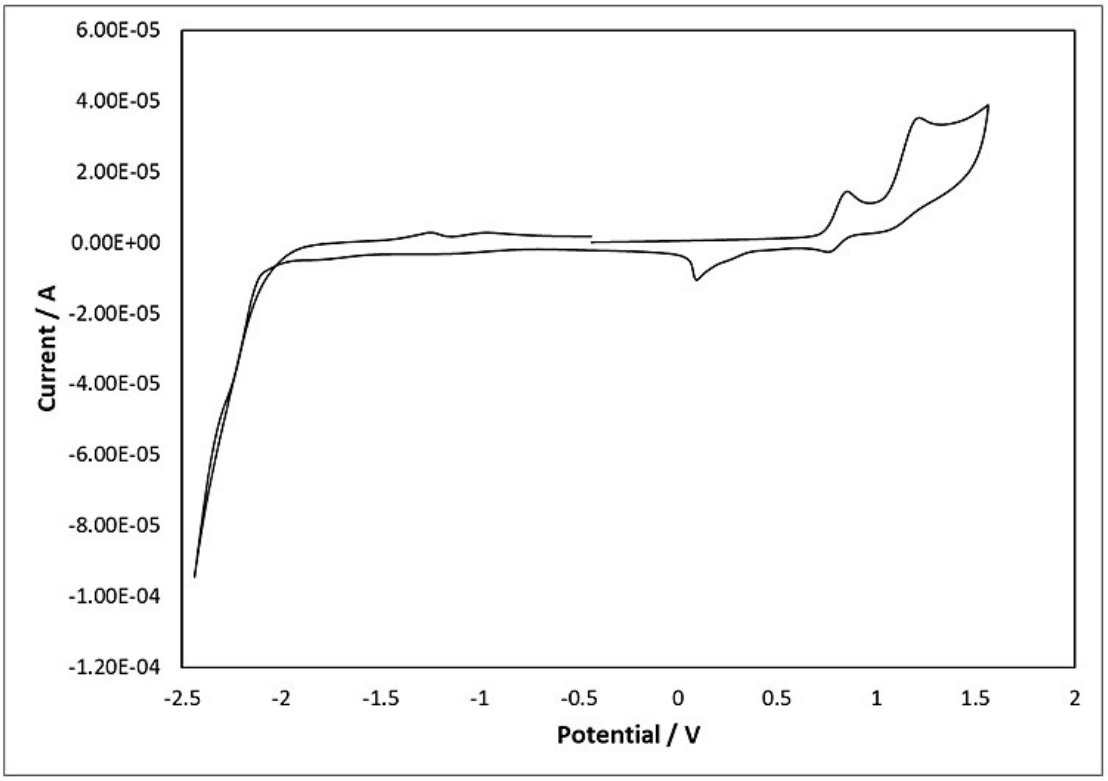

Fig. S24 Cyclic voltammogram of a CH_2Cl_2 solution of [Cu(POP)(2-Etphen)][PF_6] (vs. Fc^+/Fc, [$n$$Bu_4N$][$PF_6$] supporting electrolyte, scan rate = 0.1 V s^{-1}).

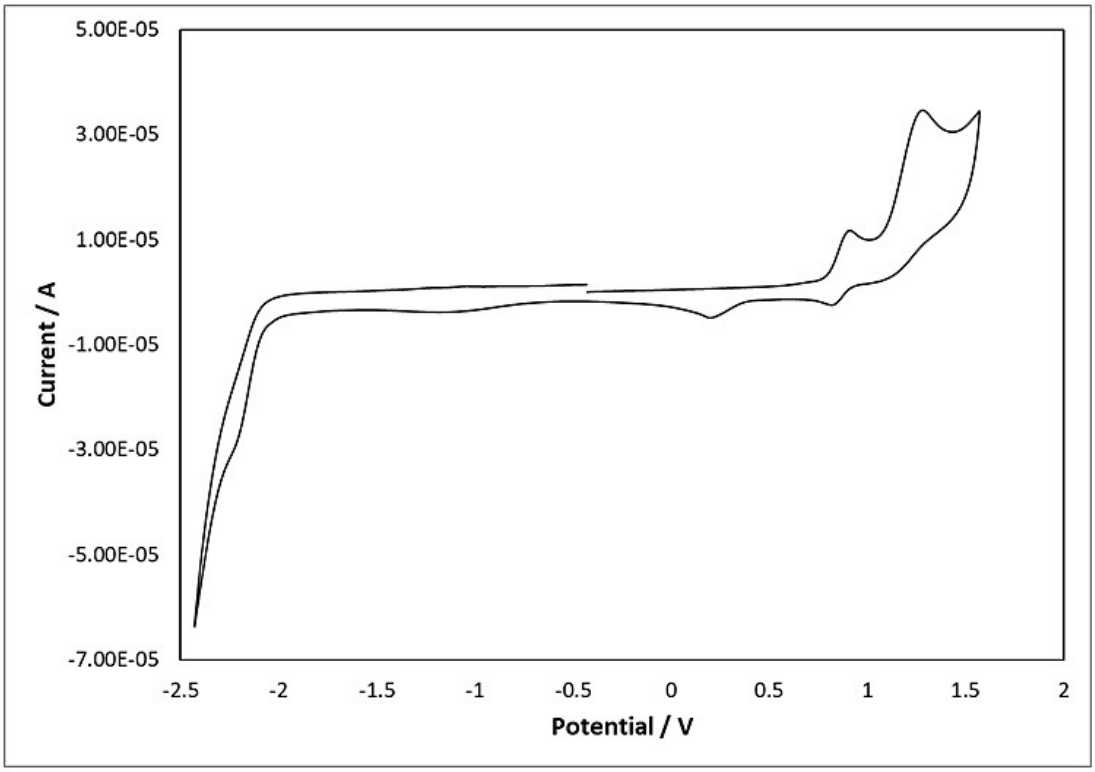

Fig. S25 Cyclic voltammogram of a CH_2Cl_2 solution of [Cu(xantphos)(2-Etphen)][PF_6] (vs. Fc^+/Fc, [$n$$Bu_4N$][$PF_6$] supporting electrolyte, scan rate = 0.1 V s^{-1}).

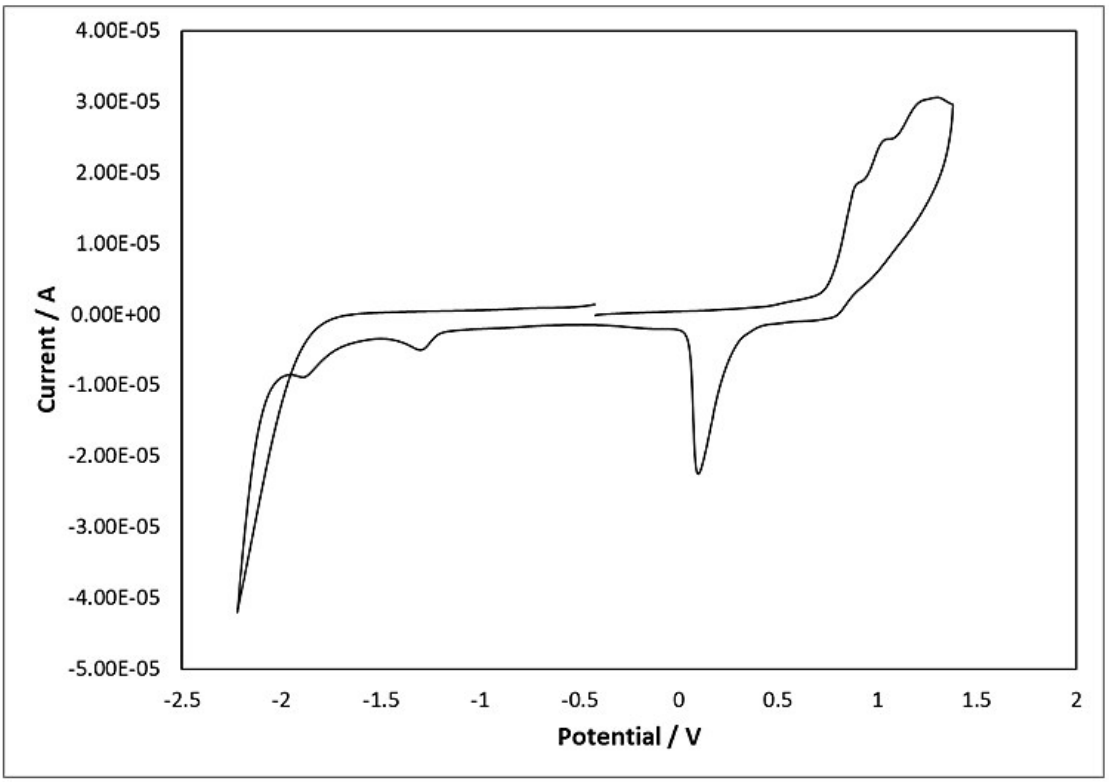

Fig. S26 Cyclic voltammogram of a CH_2Cl_2 solution of [Cu(POP)(6-*t*Bubpy)][PF_6] (vs. Fc^+/Fc, [$n$$Bu_4N$][$PF_6$] supporting electrolyte, scan rate = 0.1 V s^{-1}).

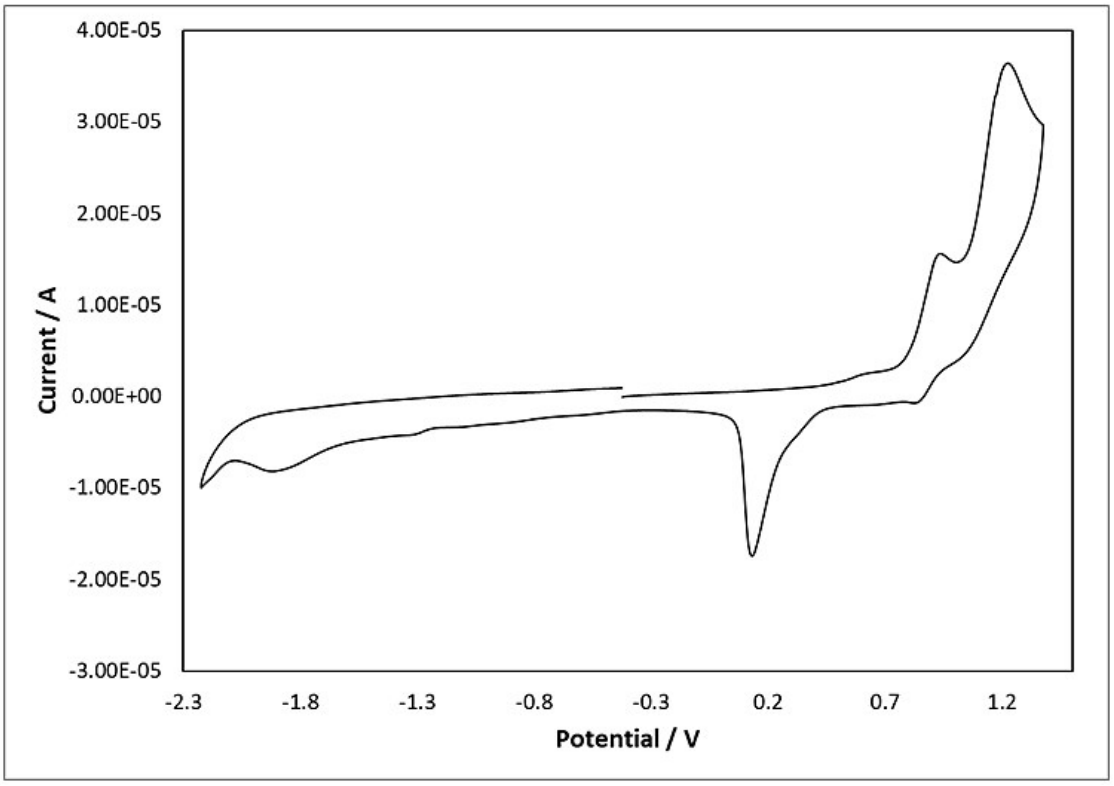

Fig. S27 Cyclic voltammogram of a CH_2Cl_2 solution of [Cu(xantphos)(6-*t*Bubpy)][PF_6] (vs. Fc^+/Fc, [$n$$Bu_4N$][$PF_6$] supporting electrolyte, scan rate = 0.1 V s^{-1}).

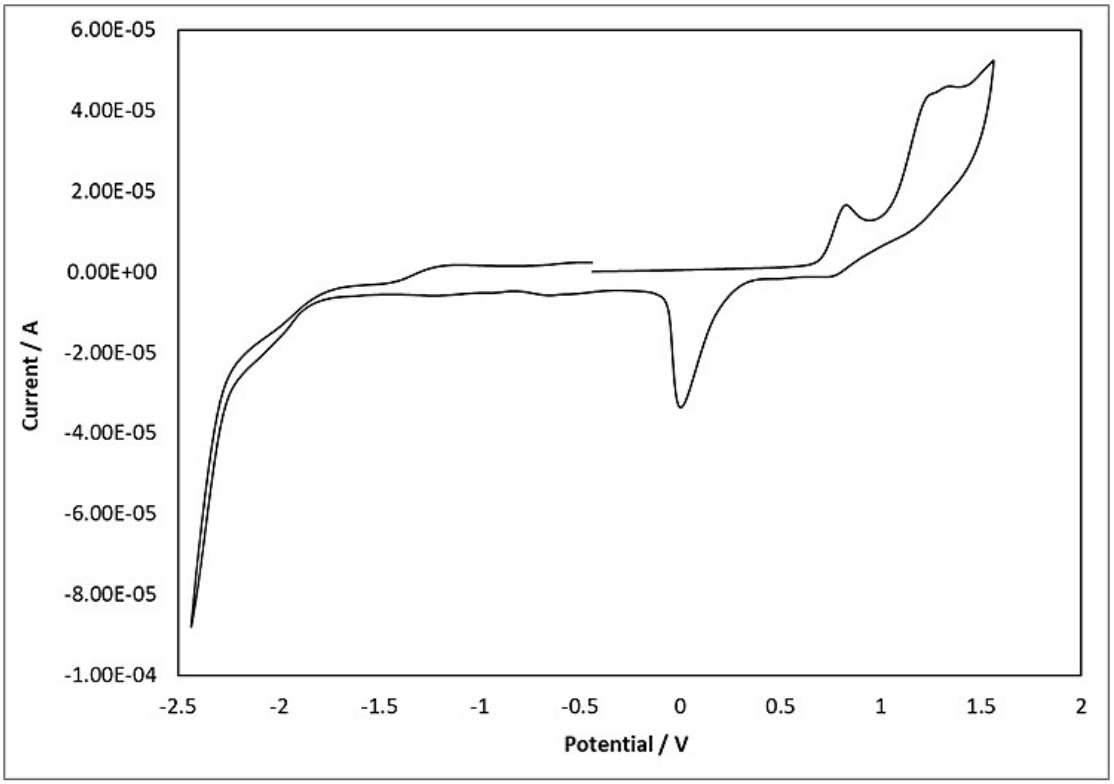

Fig. S28 Cyclic voltammogram of a CH_2Cl_2 solution of [Cu(POP)(4,5,6-Me_3bpy)][PF_6] (vs. Fc^+/Fc, [$n$$Bu_4$N][$PF_6$] supporting electrolyte, scan rate = 0.1 V s^{-1}).

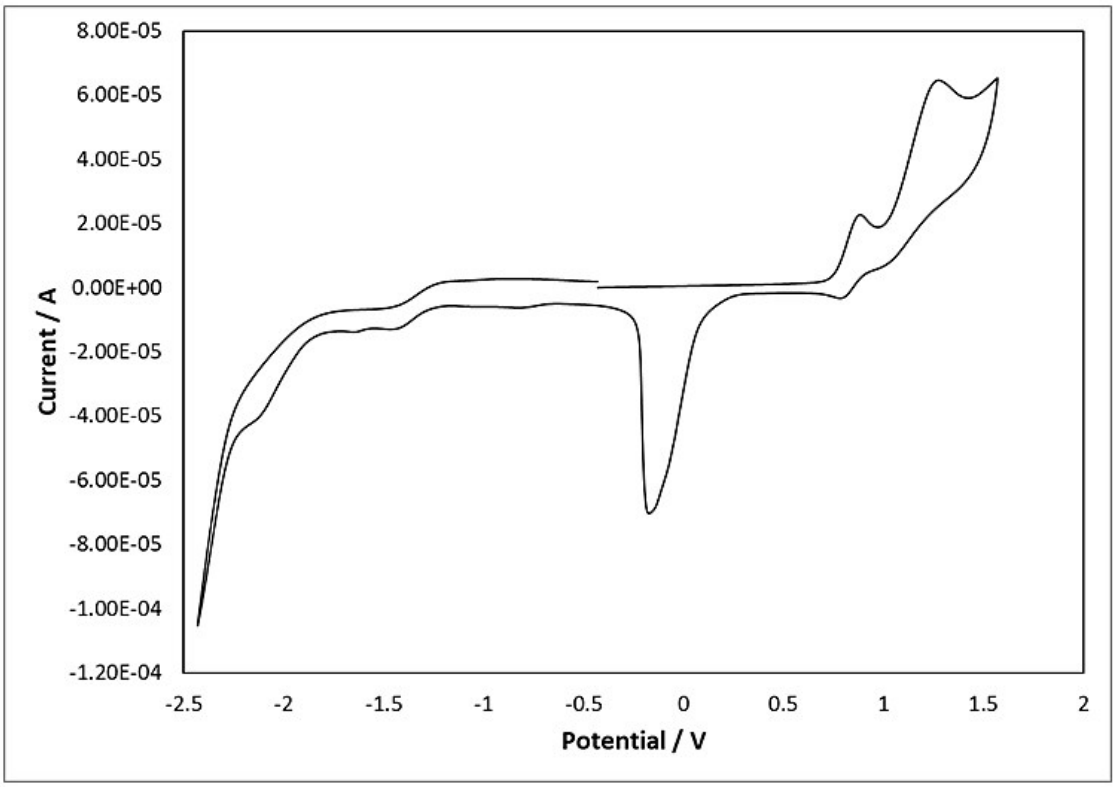

Fig. S29 Cyclic voltammogram of a CH_2Cl_2 solution of [Cu(xantphos)(4,5,6-Me_3bpy)][PF_6] (vs. Fc^+/Fc, [$n$$Bu_4$N][$PF_6$] supporting electrolyte, scan rate = 0.1 V s^{-1}).

Table S1. Selected structural parameters calculated at the B3LYP-D3/(def2-SVP+def2-TZVP) level in CH_2Cl_2 solution for the $[Cu(P\hat{}P)(N\hat{}N)]^+$ complexes in their electronic ground state S_0. The angle formed by the P–Cu–P and N–Cu–N planes (last column) is reported for both the S_0 and T_1 (within parentheses) states at their respective optimized geometries.

Complex	Cu–P bond length (Å)	Cu–N bond length (Å)	P–Cu–P chelating angle (°)	N–Cu–N chelating angle (°)	P–Cu–P/N–Cu–N angle (°)
$[Cu(POP)(bpy)]^+$	2.284; 2.246	2.069; 2.096	113.74	80.10	80.25 (59.31)
$[Cu(xantphos)(bpy)]^+$	2.270; 2.269	2.068; 2.104	114.40	79.75	86.94 (57.42)
$[Cu(POP)(5,5'\text{-}Me_2bpy)]^+$	2.247; 2.288	2.070; 2.096	113.65	80.16	79.51 (59.01)
$[Cu(xantphos)(5,5'\text{-}Me_2bpy)]^+$	2.268; 2.271	2.065; 2.109	114.07	79.76	86.01 (57.00)
$[Cu(POP)(6\text{-}t\text{Bubpy})]^+$	2.317; 2.278	2.206; 2.085	113.25	78.33	80.64 (68.35)
$[Cu(xantphos)(6\text{-}t\text{Bubpy})]^+$	2.317; 2.284	2.209; 2.084	112.73	78.90	85.55 (76.72)
$[Cu(POP)(4,5,6\text{-}Me_3bpy)]^+$	2.268; 2.281	2.107; 2.085	113.14	79.86	79.34 (60.96)
$[Cu(xantphos)(4,5,6\text{-}Me_3bpy)]^+$	2.278; 2.281	2.107; 2.088	113.71	79.89	84.20 (65.54)
$[Cu(POP)(2\text{-}Etphen)]^+$	2.270; 2.280	2.102; 2.103	113.41	80.71	83.30 (61.53)
$[Cu(xantphos)(2\text{-}Etphen)]^+$	2.275; 2.284	2.103; 2.109	113.66	80.59	86.66 (67.21)

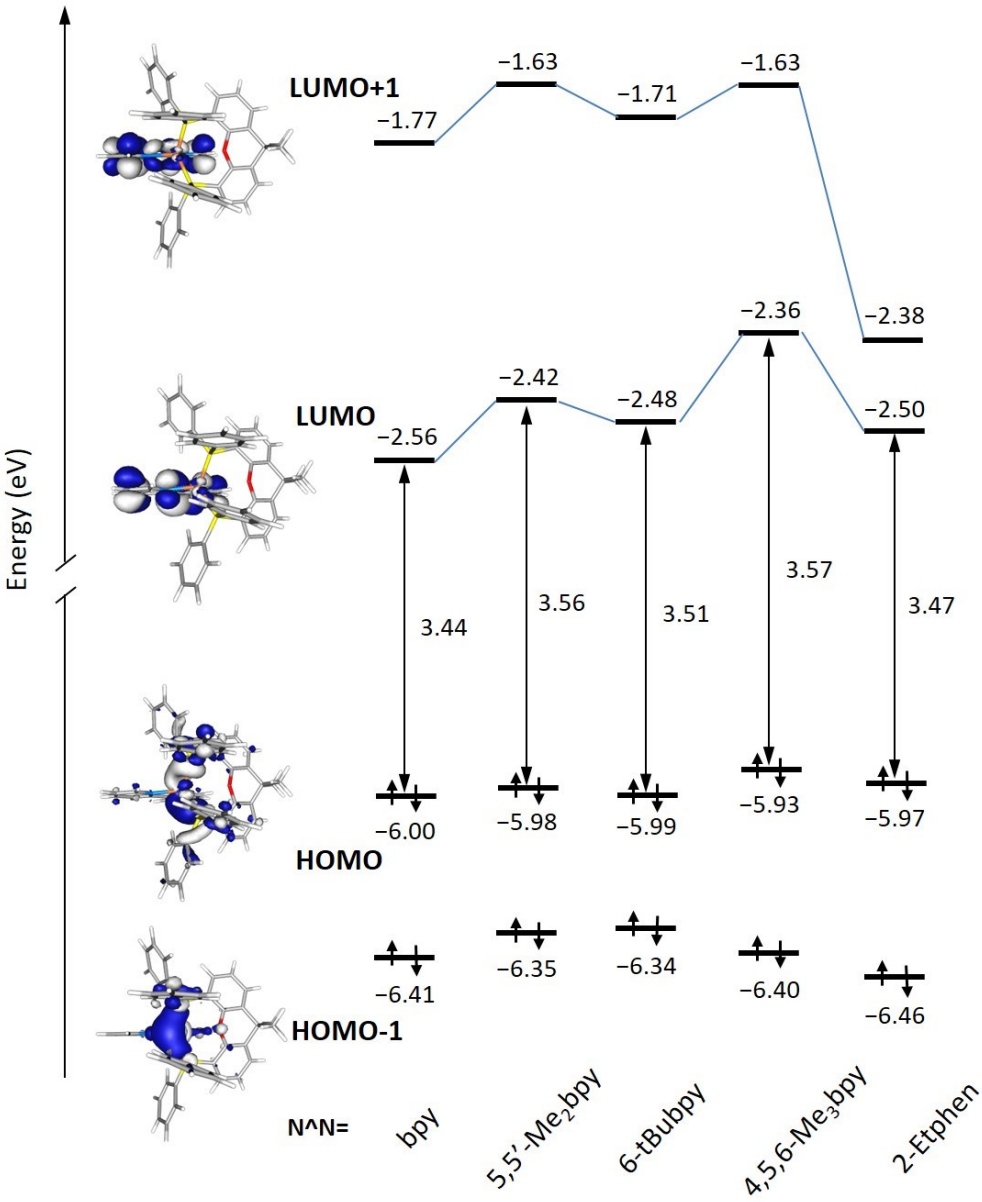

Fig. S30 Energy diagram showing the energies calculated for the HOMO−1, HOMO, LUMO and LUMO+1 of the [Cu(xantphos)(N^N)]$^+$ complexes. The HOMO−LUMO energy gap is also quoted. Isovalue contour plots (±0.03 a.u.) are shown for the reference complex [Cu(xantphos)(bpy)]$^+$.

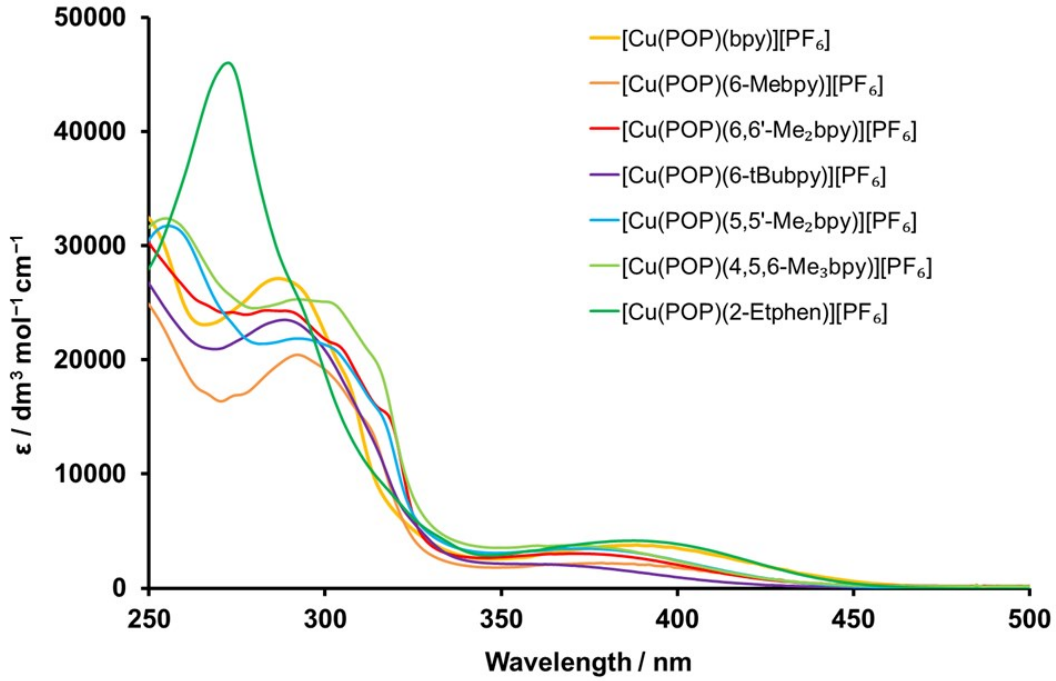

Fig. S31 Solution absorption spectra of the [Cu(POP)(N^N)][PF_6] complexes (CH_2Cl_2, 2.5 × 10^{-5} mol dm^{-3}).

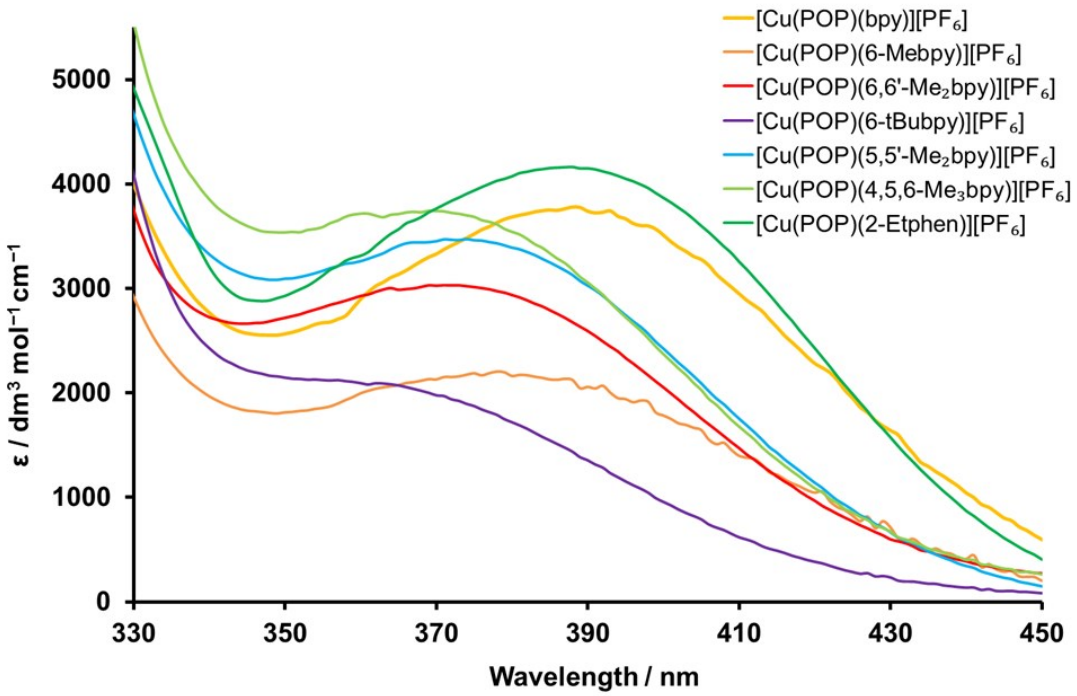

Fig. S32 Zoom into the low-energy MLCT region of the solution absorption spectra of the [Cu(POP)(N^N)][PF_6] complexes (CH_2Cl_2, 2.5 × 10^{-5} mol dm^{-3}).

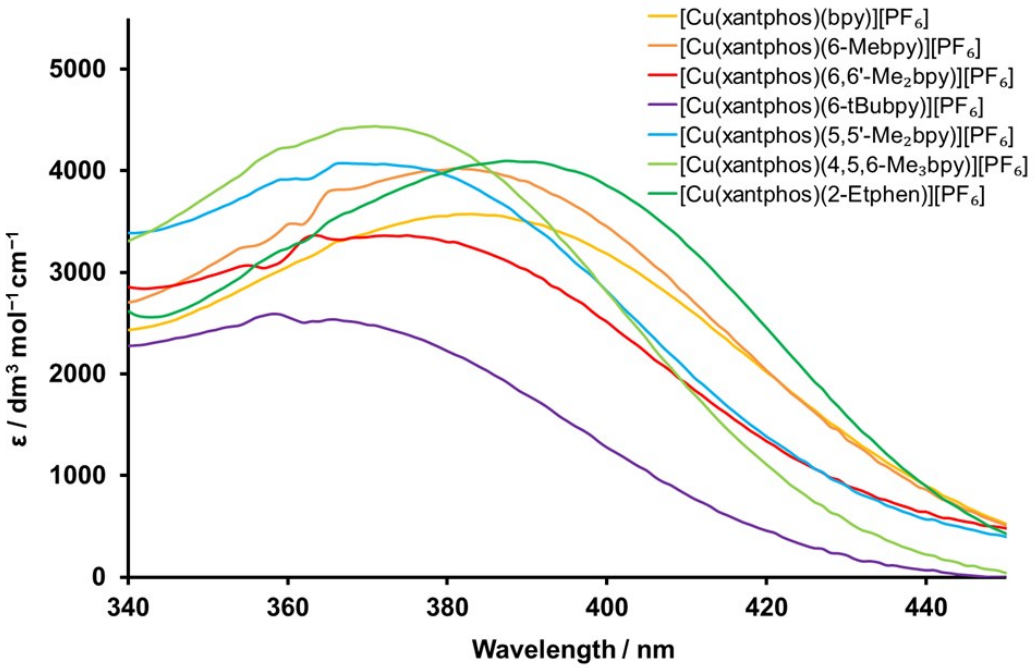

Fig. S33. Zoom into the MLCT region of the solution absorption spectra of the [Cu(xantphos)(N^N)][PF_6] complexes (CH_2Cl_2, 2.5 × 10^{-5} mol dm^{-3}).

Table S2. Absorption maxima and respective extinction coefficients of the MLCT region of the complexes in solution (CH_2Cl_2, 2.5 × 10^{-5} mol dm^{-3}).

Complex	λ_{abs}^{max} [nm]	ε [dm^3 cm^{-1} mol^{-1}]
[Cu(POP)(bpy)]$^+$	388	3780
[Cu(xantphos)(bpy)]$^+$	383	3574
[Cu(POP)(6-Mebpy)]$^+$	378	2204
[Cu(xantphos)(6-Mebpy)]$^+$	381	4024
[Cu(POP)(6,6'-Me_2bpy)]$^+$	371	3031
[Cu(xantphos)(6,6'-Me_2bpy)]$^+$	375	3363
[Cu(POP)(5,5'-Me_2bpy)]$^+$	374	3473
[Cu(xantphos)(5,5'-Me_2bpy)]$^+$	367	4074
[Cu(POP)(6-*t*Bubpy)]$^+$	362	2093
[Cu(xantphos)(6-*t*Bubpy)]$^+$	366	2537
[Cu(POP)(4,5,6-Me_3bpy)]$^+$	369	3744
[Cu(xantphos)(4,5,6-Me_3bpy)]$^+$	371	4438
[Cu(POP)(2-Etphen)]$^+$	390	4150
[Cu(xantphos)(2-Etphen)]$^+$	388	4096

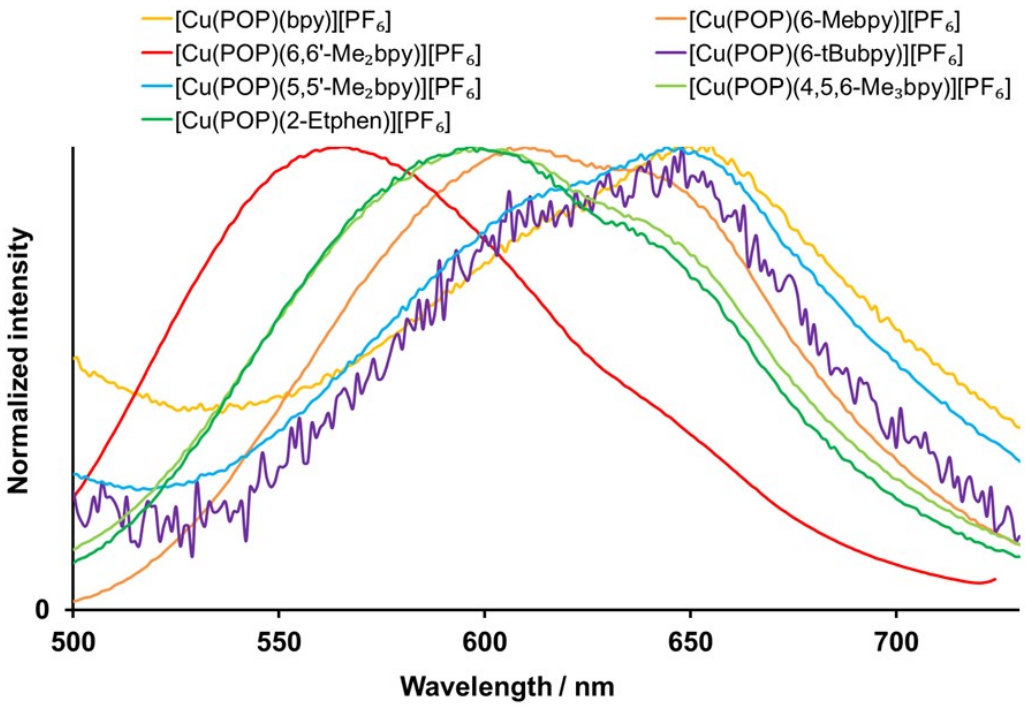

Fig. S34 Normalized solution emission spectra of the [Cu(POP)(N^N)][PF_6] complexes (CH_2Cl_2, 2.5 × 10^{-5} mol dm^{-3}). For λ_{exc} see Table 4.

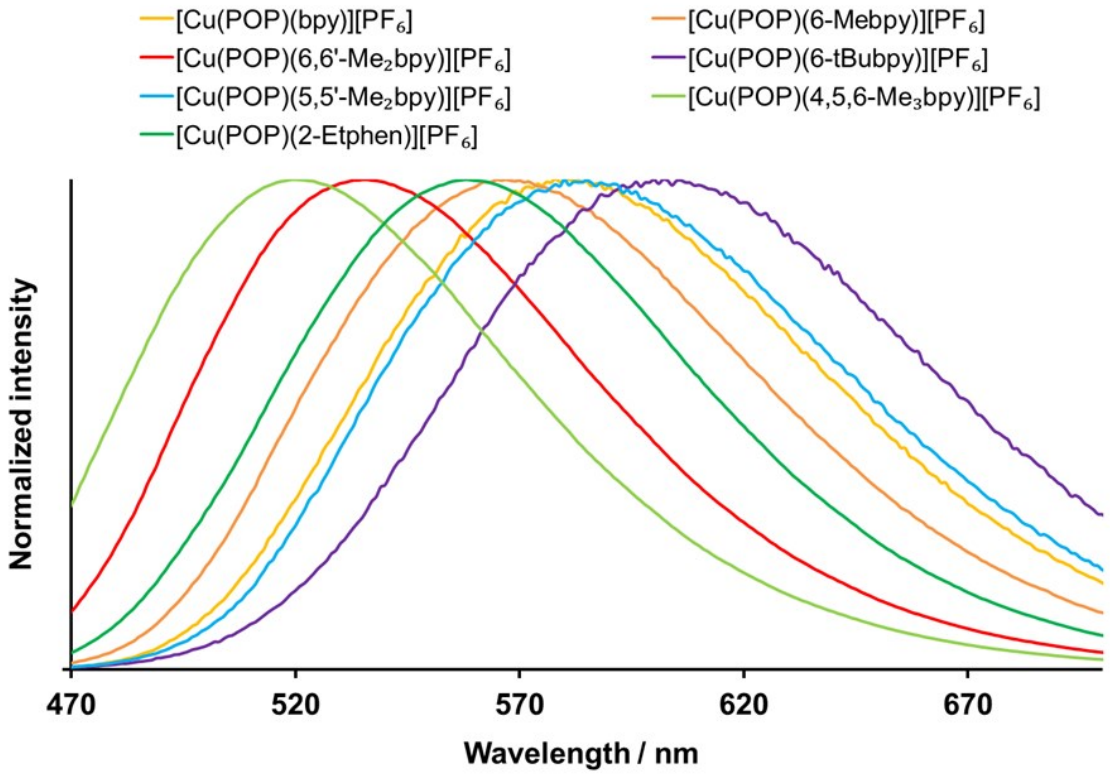

Fig. S35 Normalized emission spectra of solid [Cu(POP)(N^N)][PF_6] complexes, λ_{exc} = 365 nm.

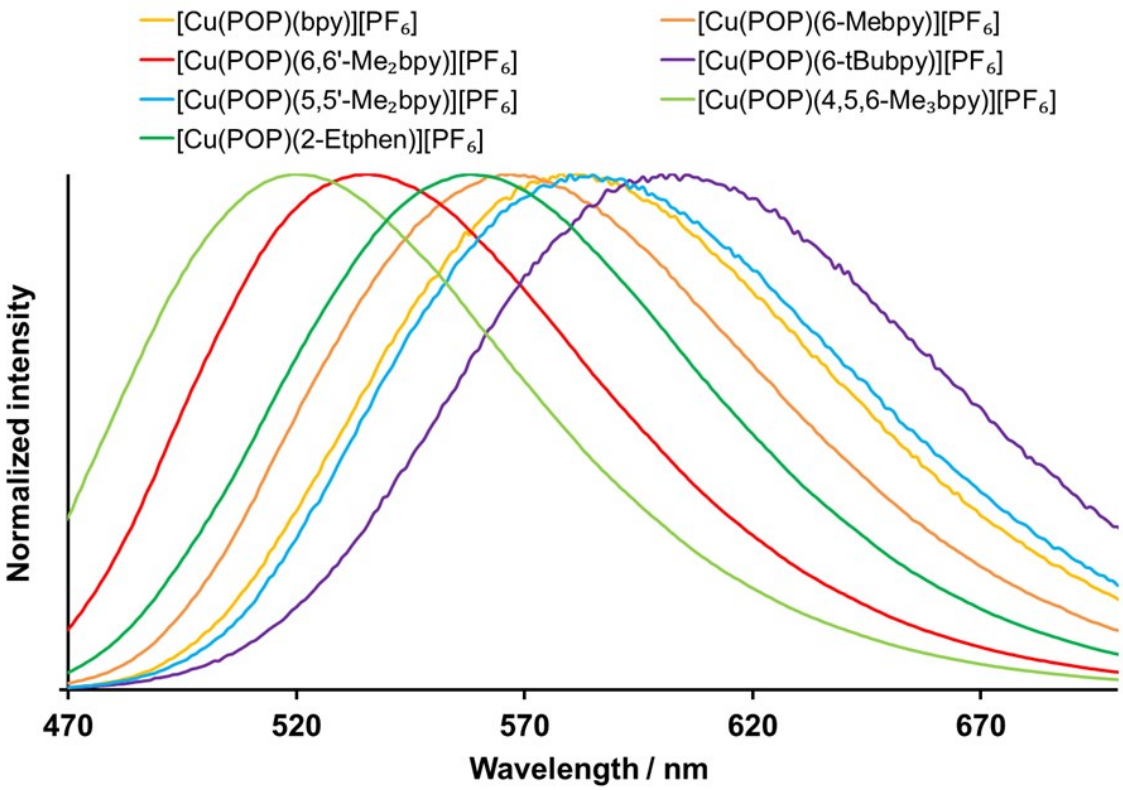

Fig. S36 Normalized emission spectra of [Cu(POP)(N^N)][PF_6] complexes in Me-THF at 77 K, λ_{exc} = 410 nm.

Table S3. Radiative and non-radiative decay rates, k_r and k_{nr} of the [Cu(POP)(N^N)][PF_6] complexes. The following formula were used for calculation: k_r = PLQY/$\tau_{1/2}$ and PLQY = $k_r/(k_r+k_{nr})$.

Complex cation	CH_2Cl_2 solution, non-deaerated [a]				CH_2Cl_2 solution, deaerated [a]				Powder[b]			
	PLQY [%]	τ [ns]	k_r [ns^{-1}]	kn_r [ns^{-1}]	PLQY [%]	τ [ns]	k_r [ns^{-1}]	kn_r [ns^{-1}]	PLQY [%]	τ [µs]	k_r [ns^{-1}]	kn_r [ns^{-1}]
[Cu(POP)(bpy)]$^+$	0.4	43	9.3E-05	2.3E-02	0.5	46	1.1E-04	2.2E-02	3.0	1.5	20.0	646.7
[Cu(xantphos)(bpy)]$^+$	0.5	75	6.7E-05	1.3E-02	0.5	104	4.8E-05	9.6E-03	1.7	1.3	13.1	756.2
[Cu(POP)(6-Mebpy)]$^+$	0.6	126	4.8E-05	7.9E-03	1.2	172	7.0E-05	5.7E-03	9.5	2.6	36.5	348.1
[Cu(xantphos)(6-Mebpy)]$^+$	1	272	3.7E-05	3.6E-03	1.8	784	2.3E-05	1.3E-03	33.8	9.7	34.8	68.2
[Cu(POP)(6,6'-Me_2bpy)]$^+$	1.3	310	4.2E-05	3.2E-03	13.8	4032	3.4E-05	2.1E-04	43.2	10.5	41.1	54.1
[Cu(xantphos)(6,6'-Me_2bpy)]$^+$	1.6	451	3.5E-05	2.2E-03	10	3406	2.9E-05	2.6E-04	37.3	11.4	32.7	55.0
[Cu(POP)(5,5'-Me_2bpy)]$^+$	0.5	57	8.8E-05	1.7E-02	0.7	108	6.5E-05	9.2E-03	2.7	2.3	11.7	423.0
[Cu(xantphos)(5,5'-Me_2bpy)]$^+$	0.4	153	2.6E-05	6.5E-03	0.9	338	2.7E-05	2.9E-03	6.3	5.1	12.4	183.7
[Cu(POP)(6-*t*Bubpy)]$^+$	0.5	39	1.3E-04	2.6E-02	0.5	45	1.1E-04	2.2E-02	1.1	0.4	27.5	2472.5
[Cu(xantphos)(6-*t*Bubpy)]$^+$	0.4	76	5.3E-05	1.3E-02	0.5	93	5.4E-05	1.1E-02	9.6	3.3	29.1	273.9
[Cu(POP)(4,5,6-Me_3bpy)]$^+$	1	202	5.0E-05	4.9E-03	1.5	730	2.1E-05	1.3E-03	42.7	9.3	45.9	61.6
[Cu(xantphos)(4,5,6-Me_3bpy)]$^+$	0.9	228	3.9E-05	4.3E-03	3.3	1595	2.1E-05	6.1E-04	58.8	9.8	60.0	42.0
[Cu(POP)(2-Etphen)]$^+$	0.8	240	3.3E-05	4.1E-03	6	2401	2.5E-05	3.9E-04	27.5	8.7	31.6	83.3
[Cu(xantphos)(2-Etphen)]$^+$	0.9	262	3.4E-05	3.8E-03	9.6	4987	1.9E-05	1.8E-04	9.8	10.2	9.6	88.4

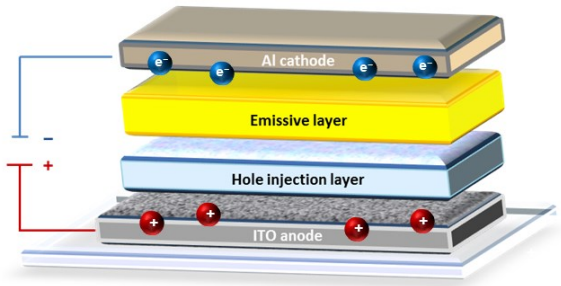

Fig. S37. Schematic representation of a LEC in the configuration used in this work.

Table S4. Performance of ITO/PEDOT:PSS/[Cu(P^P)(N^N)][PF_6]:[Emim][PF_6] 4:1 molar ratio/Al LECs measured using a pulsed current driving (average current density 50 or 100 A m^{-2}, 1 kHz, 50% duty cycle, block wave).

Complex	J_{avg} [A m^{-2}]	t_{on} [a] [min]	Lum_0 [b] [cd m^{-2}]	Lum_{max} [c] [cd m^{-2}]	$t_{1/2}$ [d] [hours]	EQE_{max} [e] [%]	PCE_{max} [f] [lm W^{-1}]	$Efficacy_{max}$ [g] [cd A^{-1}]	λ_{EL}^{max} [h] [nm]
[Cu(POP)(5,5'-Me_2bpy)]$^+$	50	320	0	33	54.6	0.30	0.4	0.7	588
[Cu(xantphos)(5,5'-Me_2bpy)]$^+$	50	138	0	58	16.5	0.50	0.8	1.2	589
	100	19	20	130	7.7	1.20	0.9	1.3	
[Cu(POP)(6-*t*Bubpy)]$^+$	100	71	0	13	15.0	0.05	0.1	0.1	585
[Cu(xantphos)(6-*t*Bubpy)]$^+$	100	110	0	34	27.8	0.15	0.2	0.3	586

[a] Time to reach the maximum luminance. [b] Initial luminance. [c] Maximum luminance. [d] Time to reach half of the maximum luminance. [e] Maximum external quantum efficiency. [f] Maximum power conversion efficiency. [g] Maximum current efficiency. [h] Wavelength at the maximum intensity of the electroluminescence spectrum.

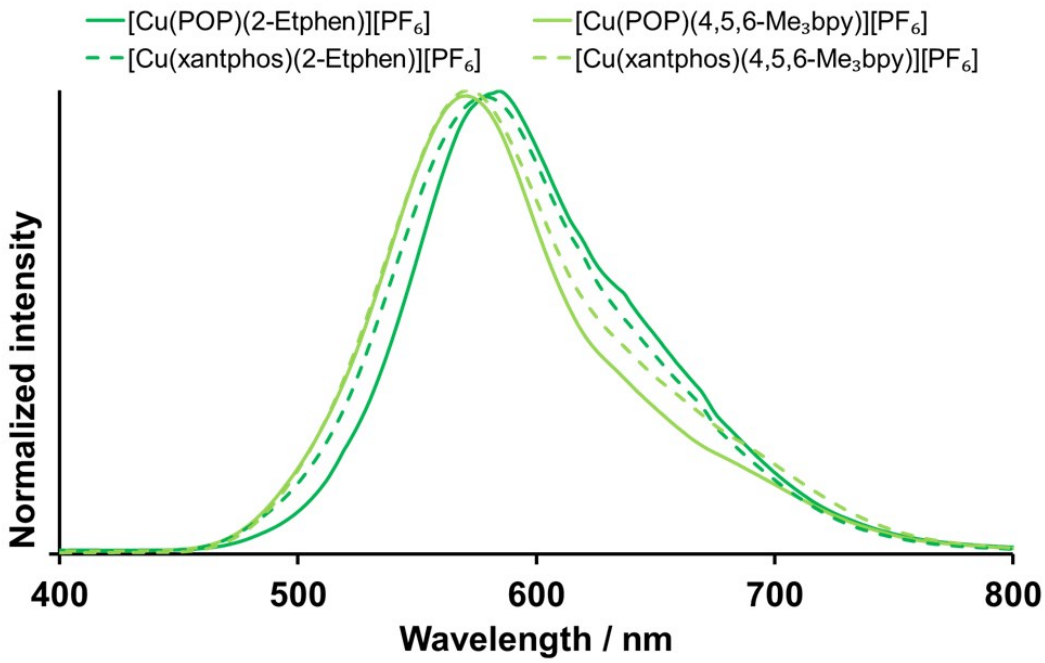

Fig. S38 Electroluminescence spectra for ITO/PEDOT:PSS/[Cu(P^P)^N^N)][PF_6]:[Emim][PF_6] 4:1 molar ratio/Al LECs measured using a pulsed current driving and under continuous operation.

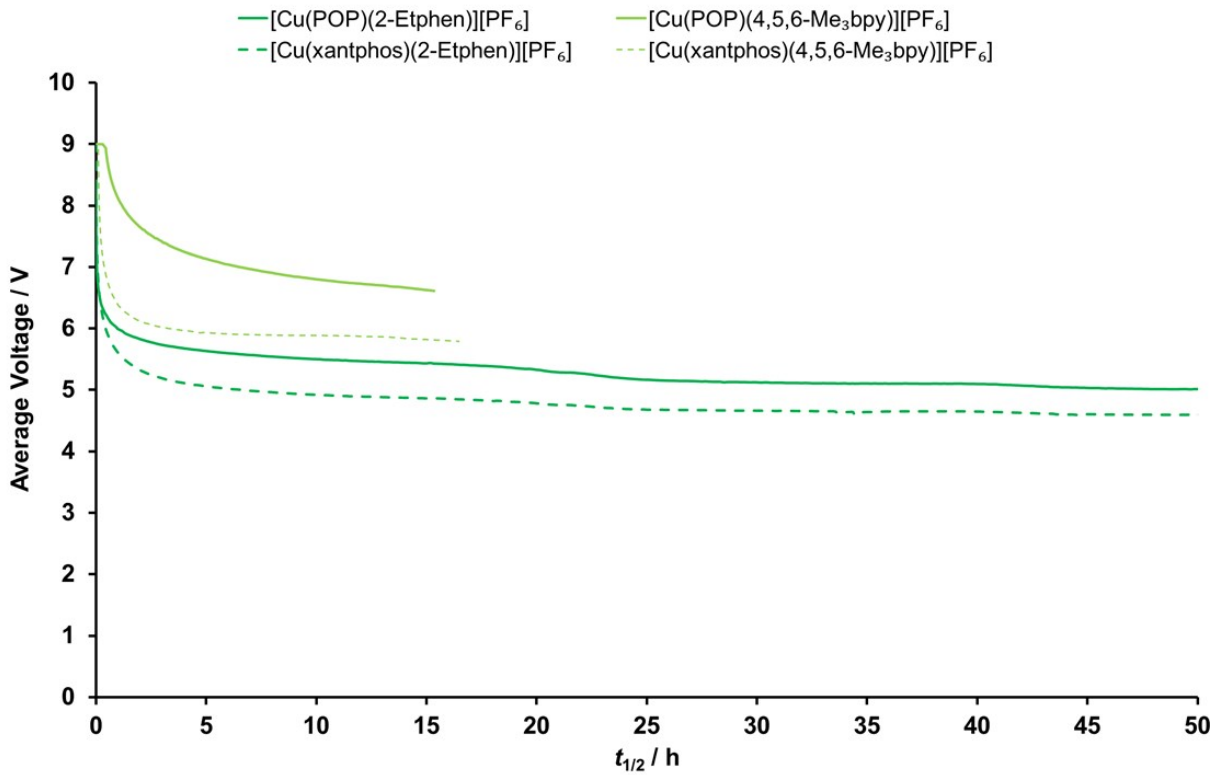

Fig. S39 Time evolution of average voltage for ITO/PEDOT:PSS/[Cu(P^P)^N^N)][PF_6]:[Emim][PF_6] 4:1 molar ratio/Al LECs measured using a pulsed current driving and under continuous operation.

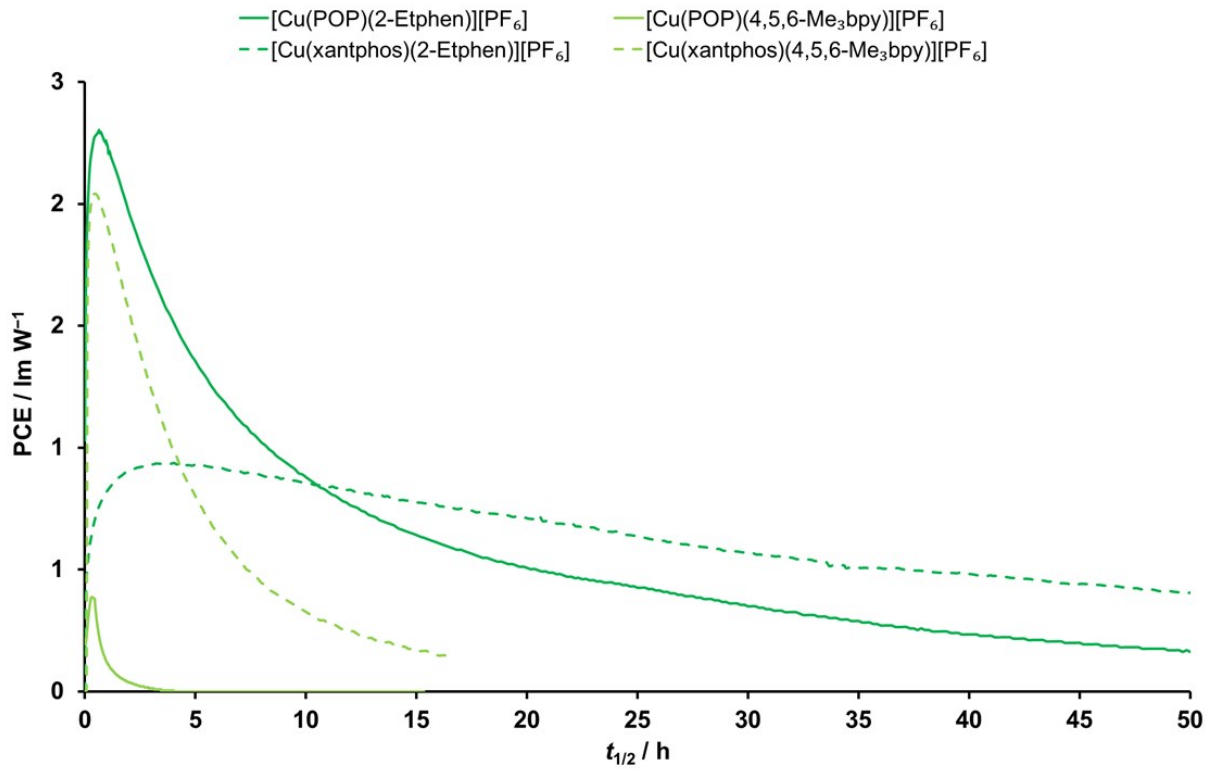

Fig. S40 Time evolution of power conversion efficiency for ITO/PEDOT:PSS/[Cu(P^P)^N^N)][PF_6]:[Emim][PF_6] 4:1 molar ratio/Al LECs measured using a pulsed current driving and under continuous operation.

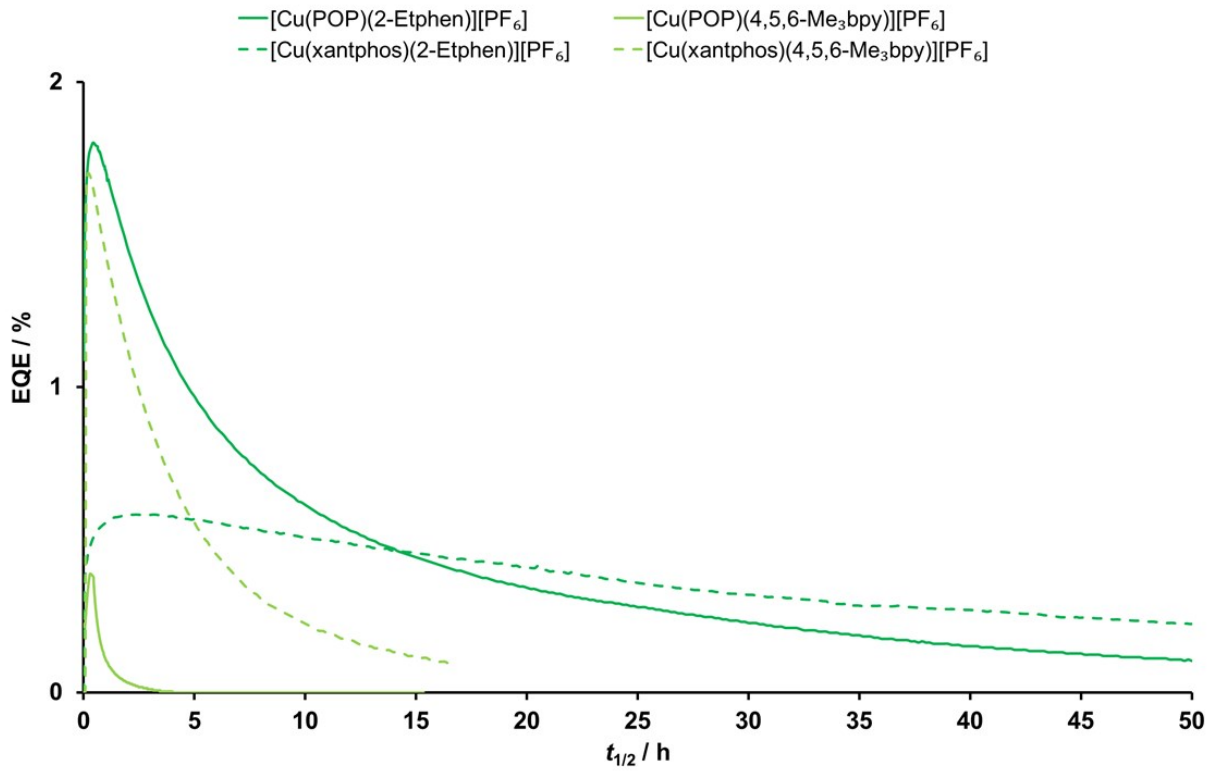

Fig. S41 Time evolution of external quantum efficiency for ITO/PEDOT:PSS/[Cu(P^P)^N^N)][PF_6]:[Emim][PF_6] 4:1 molar ratio/Al LECs measured using a pulsed current driving and under continuous operation.

References

1 Y. Sekiguchi, Y. Kanuma, K. Omodera, K. Abe, M. Hayashi, S. Yamamoto, Assignee: Taisho Pharmaceutical Co., Ltd., Japan; Arena Pharmaceutical Inc., Jpn. Kokai Tokkyo Koho (2007), JP 2007291087 A 20071108.

2 L. Hintermann, L. Xiao and A. Labonne, *Angew. Chem. Int. Ed.*, 2008, **47**, 8246.

3 G. J. Kubas, *Inorg. Synth*., 1979, **19**, 90.

4 A. Zucca, M. A. Cinellu, M. V. Pinna, S. Stoccoro, G. Minghetti, M. Manassero and M. Sansoni, *Organometallics,* 2000, **19**, 4295.

5 Y.-Q. Fang, G. S. Hanan, *Synlett.*, 2003, **6**, 852.

6 Y. Cheng, X. Han, H. Ouyang, Y. Rao, *Chem. Commun.*, 2012, **48**, 2906.

7 Bruker Analytical X-ray Systems, Inc., 2006, APEX2, version 2 User Manual, M86-E01078, Madison, WI.

8 P. W. Betteridge, J. R. Carruthers, R. I. Cooper, K. Prout and D. J. Watkin, *J. Appl. Cryst*., 2003, **36**, 1487.

9 I. J. Bruno, J. C. Cole, P. R. Edgington, M. K. Kessler, C. F. Macrae, P. McCabe, J. Pearson and R. Taylor, *Acta Crystallogr., Sect. B*, 2002, **58**, 389.

10 C. F. Macrae, I. J. Bruno, J. A. Chisholm, P. R. Edgington, P. McCabe, E. Pidcock, L. Rodriguez-Monge, R. Taylor, J. van de Streek and P. A. Wood, *J. Appl. Cryst*., 2008, **41**, 466.

11 Gaussian 16, Revision A.03, M. J. Frisch, G. W. Trucks, H. B. Schlegel, G. E. Scuseria, M. A. Robb, J. R. Cheeseman, G. Scalmani, V. Barone, G. A. Petersson, H. Nakatsuji, X. Li, M. Caricato, A. V. Marenich, J. Bloino, B. G. Janesko, R. Gomperts, B. Mennucci, H. P. Hratchian, J. V. Ortiz, A. F. Izmaylov, J. L. Sonnenberg, D. Williams-Young, F. Ding, F. Lipparini, F. Egidi, J. Goings, B. Peng, A. Petrone, T. Henderson, D. Ranasinghe, V. G. Zakrzewski, J. Gao, N. Rega, G. Zheng, W. Liang, M. Hada, M. Ehara, K. Toyota, R. Fukuda, J. Hasegawa, M. Ishida, T. Nakajima, Y. Honda, O. Kitao, H. Nakai, T. Vreven, K. Throssell, J. A. Montgomery, Jr., J. E. Peralta, F. Ogliaro, M. J. Bearpark, J. J. Heyd, E. N. Brothers, K. N. Kudin, V. N. Staroverov, T. A. Keith, R. Kobayashi, J. Normand, K. Raghavachari, A. P. Rendell, J. C. Burant, S. S. Iyengar, J. Tomasi, M. Cossi, J. M. Millam, M. Klene, C. Adamo, R. Cammi, J. W. Ochterski, R. L. Martin, K. Morokuma, O. Farkas, J. B. Foresman and D. J. Fox, Gaussian, Inc., Wallingford CT, 2016.

12 C. Lee, W. Yang and R.G. Parr, *Phys. Rev. B*, 1988, **37**, 785.

13 A. D. Becke, *J. Chem. Phys.*, 1993, **98**, 5648.

14 S. Grimme, J. Antony, S. Ehrlich and H. Krieg, *J. Chem. Phys.*, 2010, **132**, 154104.

15 S. Grimme, S. Ehrlich and L. Goerigk, *J. Comput. Chem.*, 2011, **32**, 1456.
16 F. Weigend and R. Ahlrichs, *Phys. Chem. Chem. Phys.*, 2005, **7**, 3297.
17 F. Weigend, *Phys. Chem. Chem. Phys.*, 2006, **8**, 1057.
18 M. Petersilka, U. J. Gossmann and E. K. U. Gross, *Phys. Rev. Lett.*, 1996, **76**, 1212.
19 C. Jamorski, M. E. Casida and D. R. Salahub, *J. Chem. Phys.*, 1996, **104**, 5134.
20 M. E. Casida, C. Jamorski, K. C. Casida and D. R. Salahub, *J. Chem. Phys.*, 1998, **108**, 4439.
21 J. Tomasi and M. Persico, *Chem. Rev.*, 1994, **94**, 2027.
22 C. J. Cramer and D. G. Truhlar, in *Solvent Effects and Chemical Reactivity*. O. Tapia and J. Bertrán (Eds.), Kluwer, 1996, pp. 1–80.
23 J. Tomasi, B. Mennucci and R. Cammi, *Chem. Rev.*, 2005, **105**, 2999.